Nuclear Shell Structure, Nuclear Forces and Nuclear Weak Processes

Toshio Suzuki
Nihon University, Tokyo

NORDITA 2014
Sept. 23, 2014

1. New shell-model Hamiltonians with proper **tensor forces**

- SFO: p-shell, p-sd shell
- GXPF1: pf-shell
- VMU (monopole-based universal interaction): sd-pf, p-sd

Spin modes - GT strengths - are well described.
Applications to nuclear weak processes - ν-nucleus and e-capture reactions - at stellar environments, and nucleosynthesis in supernova explosions

2. **Three-nucleon forces** and repulsive corrections in T=1 monopoles

Structure of neutron-rich isotopes: C, O, Ca
Ca isotopes: pf vs $pfg_{9/2}$

- New shell-model Hamiltonians and successful description of Gamow-Teller (GT) strengths and M1 transitions & moments
  - SFO (p-shell, p-sd shell): GT in ^{12}C, ^{14}C, M1 moments
    - Suzuki, Fujimoto, Otsuka, PR C69, (2003)
  - GXPF1J (fp-shell): GT in Fe and Ni isotopes, M1 strengths
    - Honma, Otsuka, Mizusaki, Brown, PR C65 (2002); C69 (2004)
    - Suzuki, Honma et al., PR C79, (2009)
  - VMU (monopole-based universal interaction)
    - Otsuka, Suzuki, Honma, Utsuno et al., PRL 104 (2010) 012501

＊ important roles of tensor force

Monopole terms of V_{NN}

$$V_M^T(j_1 j_2) = \frac{\sum_J (2J+1) < j_1 j_2; JT | V | j_1 j_2; JT >}{\sum_J (2J+1)}$$

$j_> - j_<$: attractive

$j_> - j_>, j_< - j_<$: repulsive

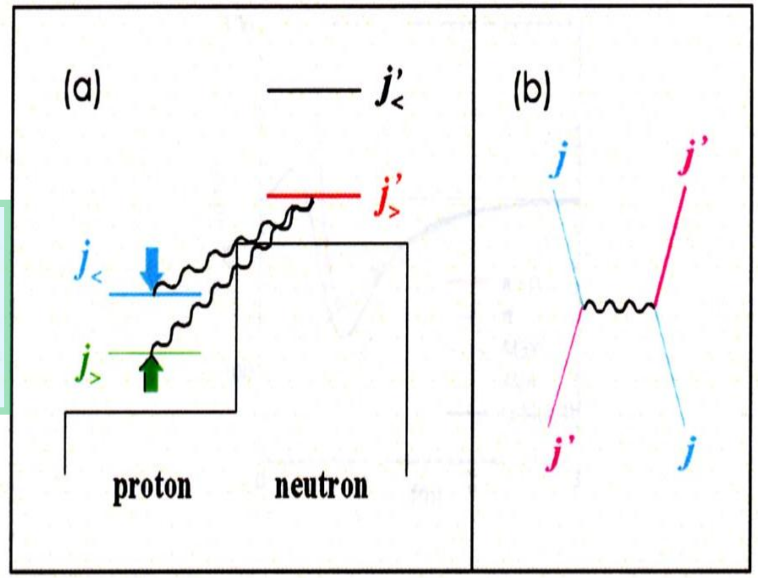

Otsuka, Suzuki, Fujimoto, Grawe, Akaishi, PRL 69 (2005)

G-matrix vs phenom. interactions

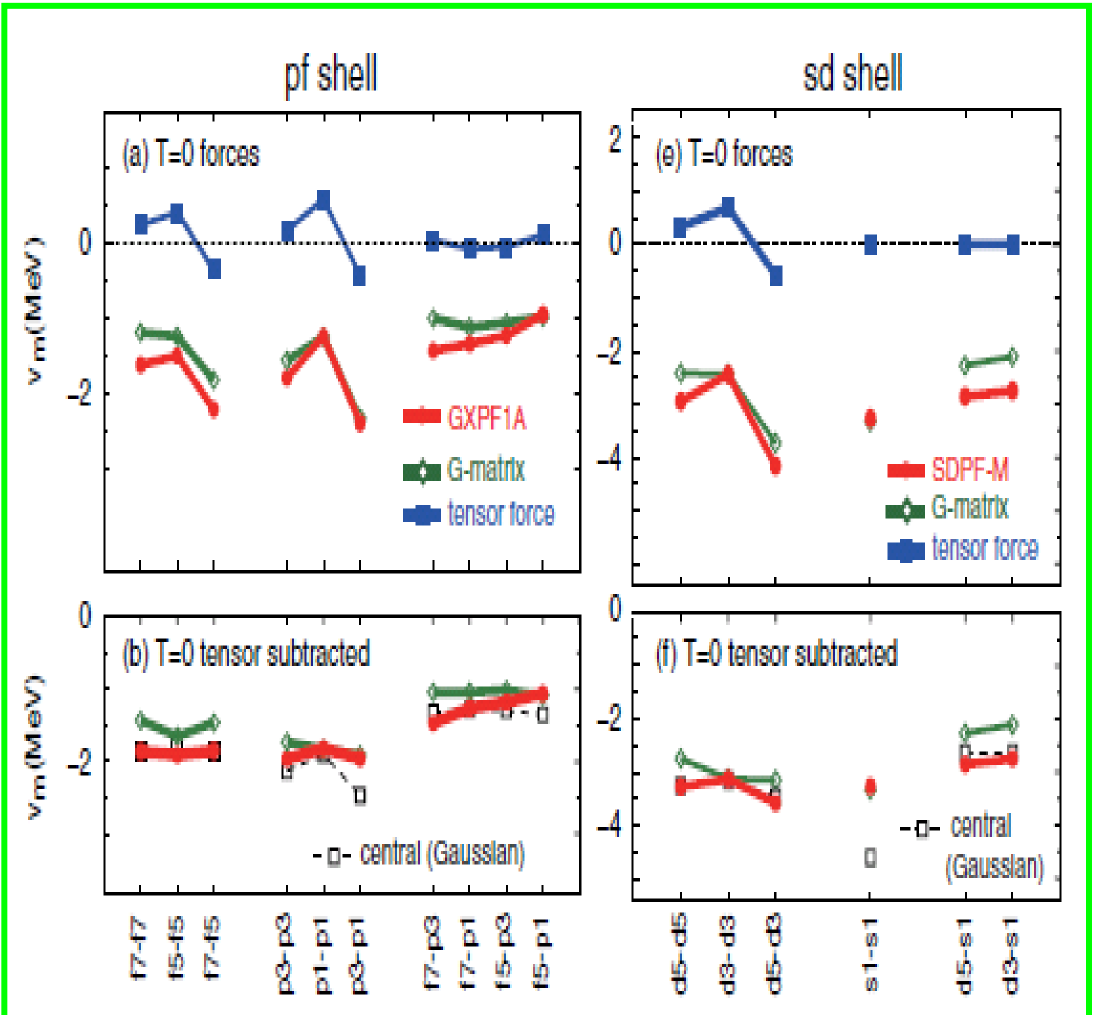

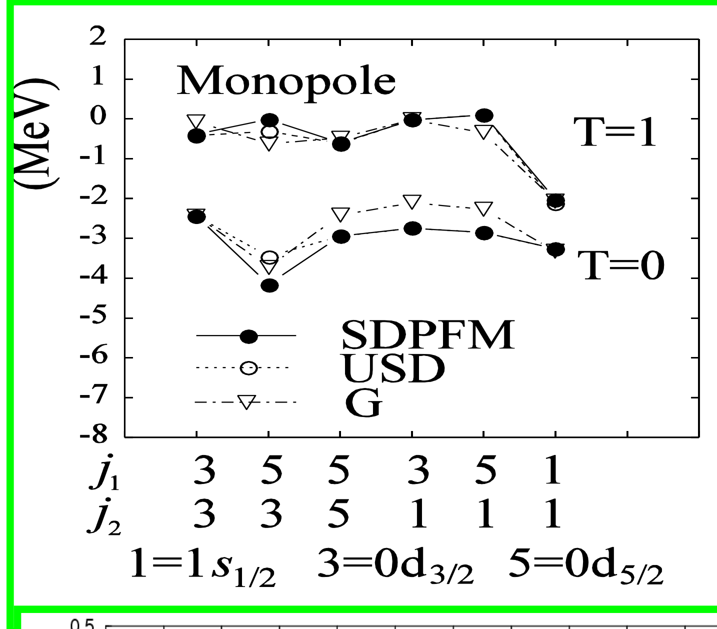

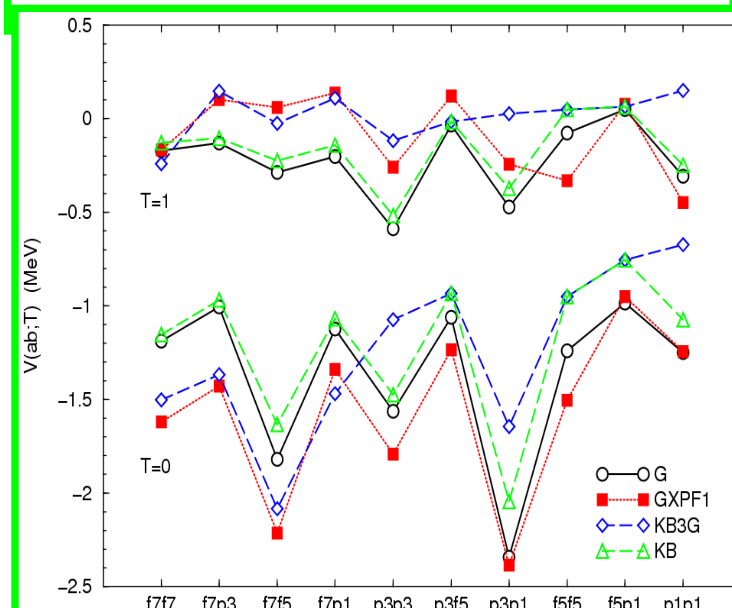

tensor force → characteristic orbit dependence: kink

more repulsion than G in T=1
more attraction than G in T=0

Monopole terms: p-sd shell

p1/2-p3/2 (T=0) monopole and
spe gap ε(p1/2)-ε(p3/2) enhanced

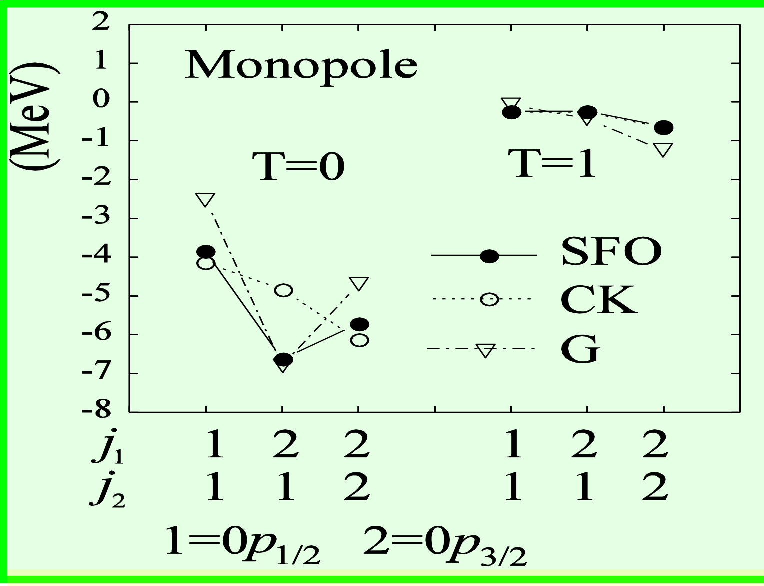

Monopole matrix elements

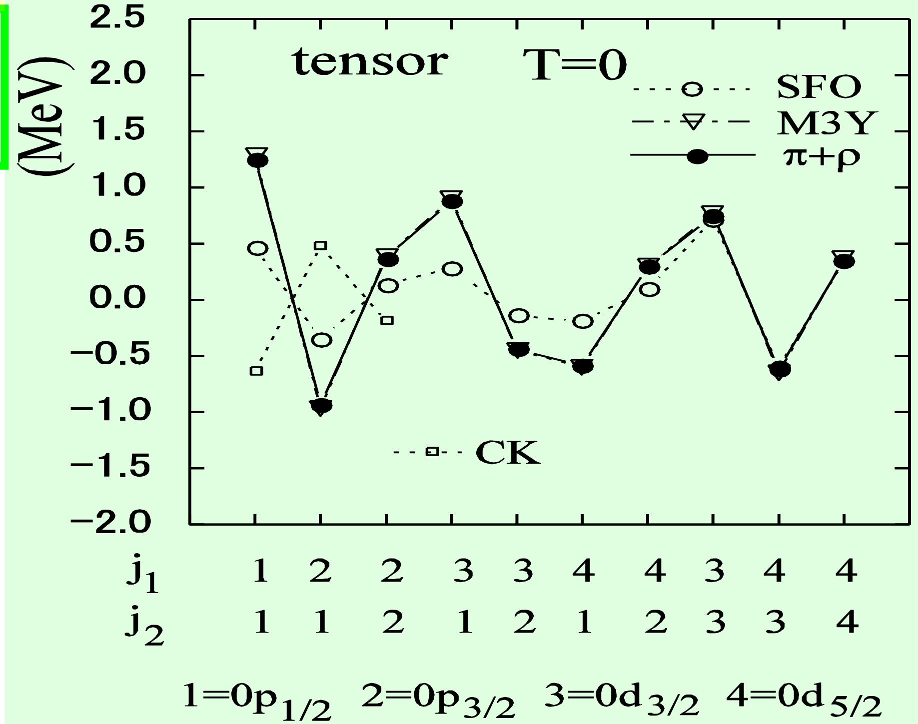

Proper shell evolutions toward drip-lines: Change of magic numbers

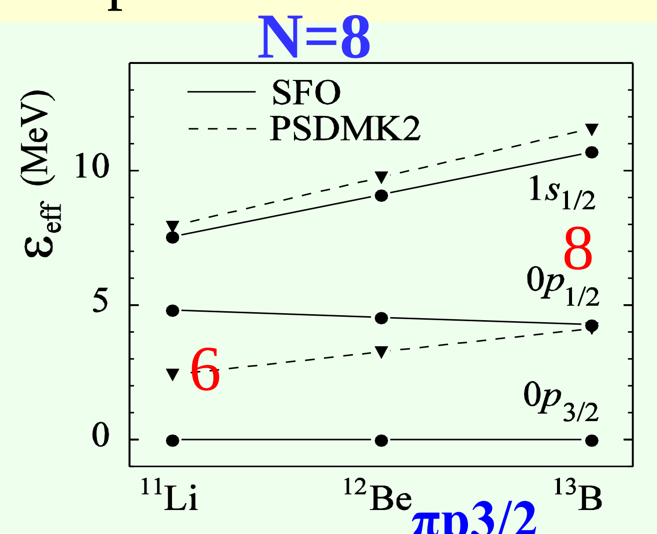

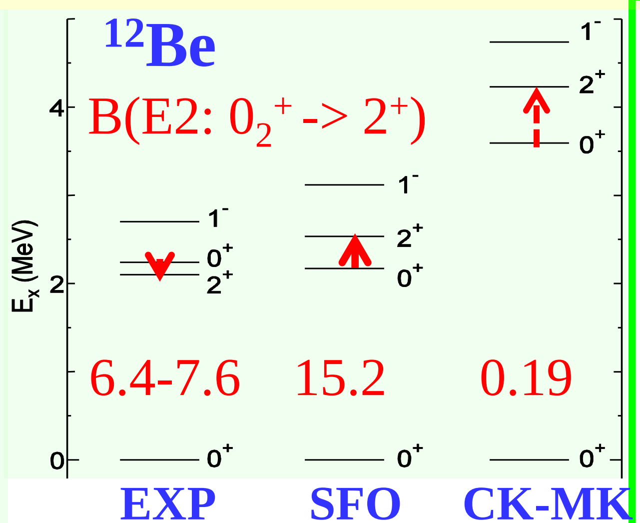

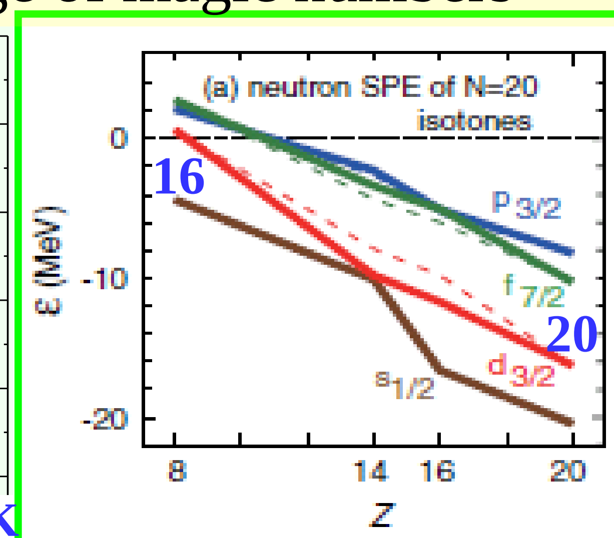

Energy levels of p-shell nuclei   SFO

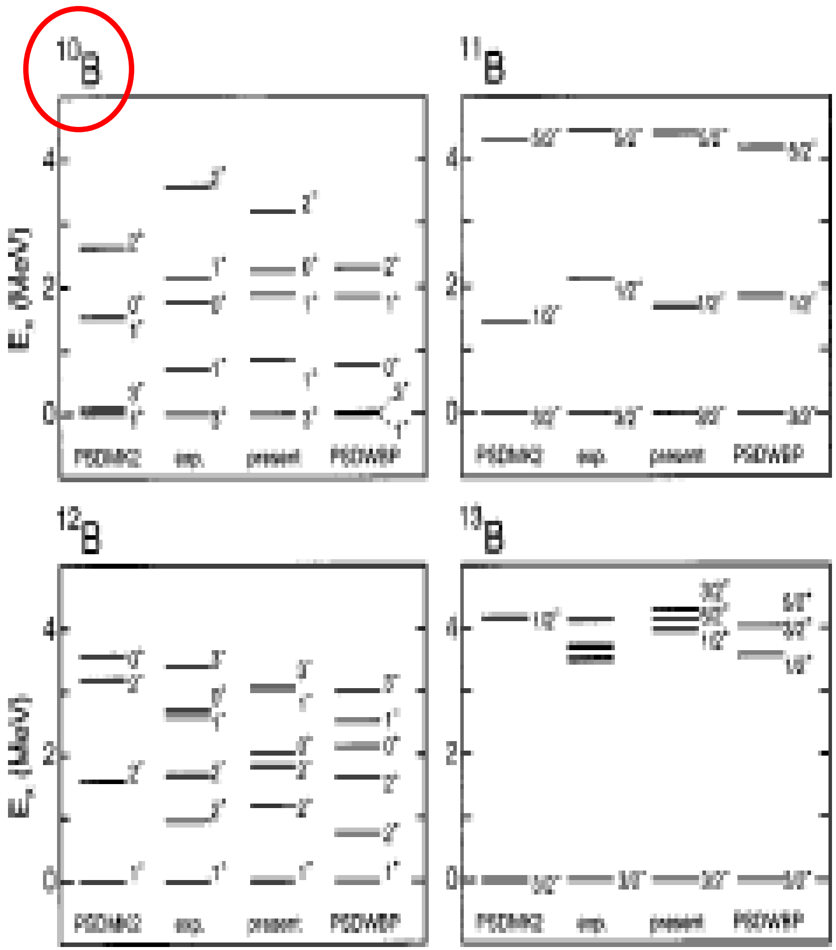

FIG. 1. Comparison of calculated and experimental energy levels for $^{10-13}$B isotopes. Calculated energy levels are obtained for the PSDMK2, and the present and the PSDWBP Hamiltonians.

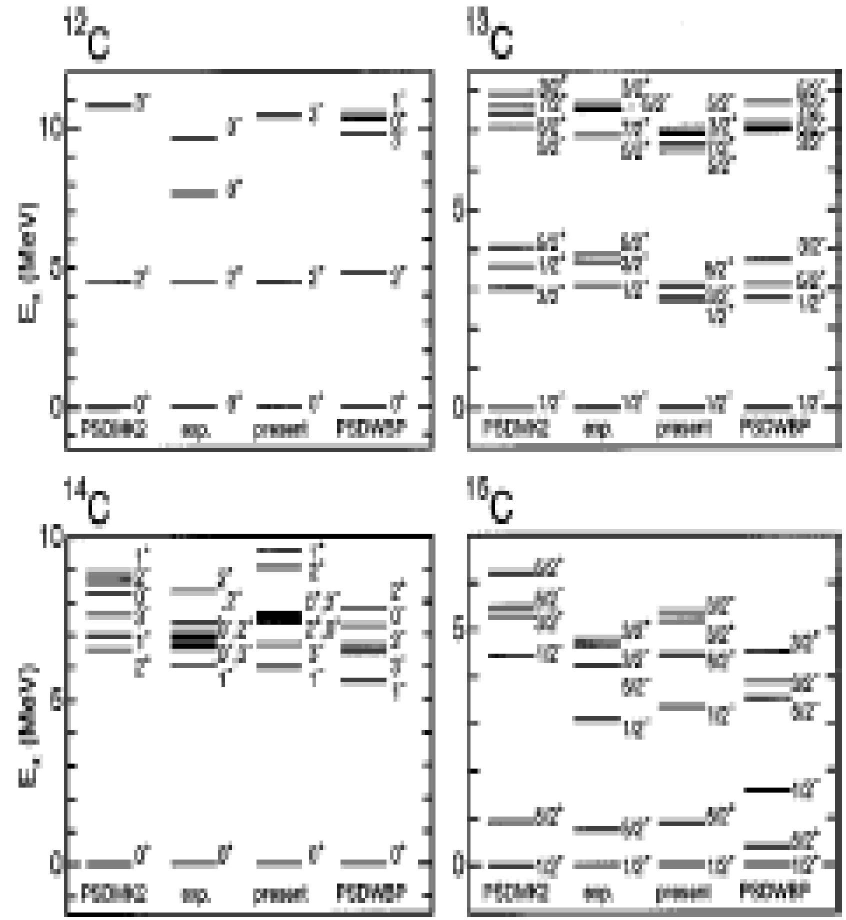

FIG. 2. Comparison of calculated and experimental energy levels for $^{12-15}$C isotopes. Calculated energy levels are obtained for the PSDMK2, and present and the PSDWBP Hamiltonians.

B(GT) values for ^{12}C -> ^{12}N

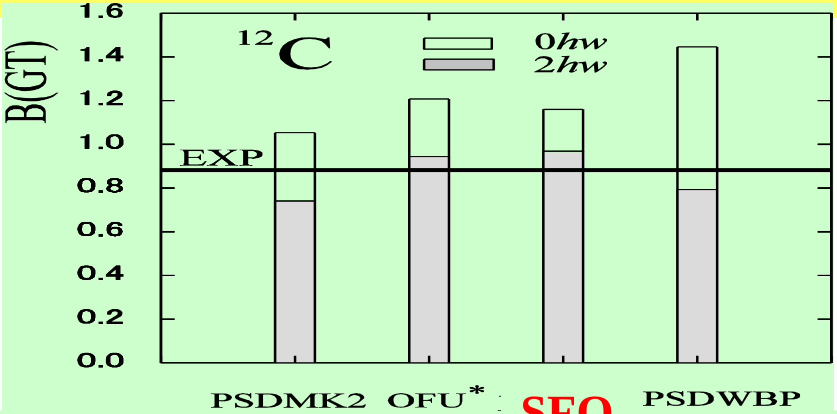

SFO

B(GT) values for ^{14}N -> ^{14}C

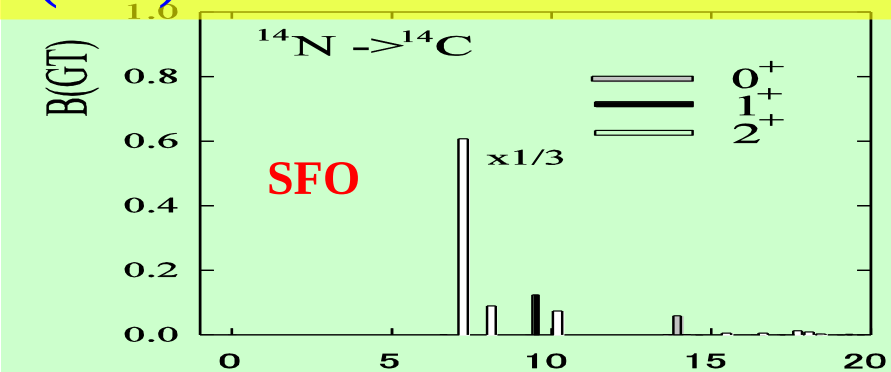

SFO

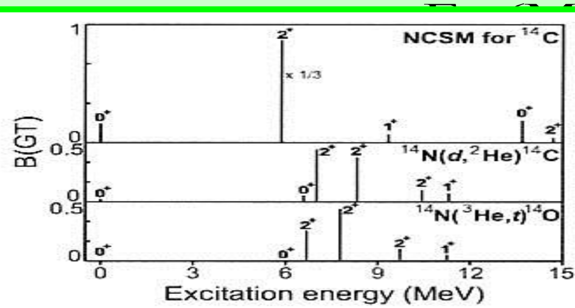

FIG. 3. Experimental B(GT) distributions, compared to the theoretical result of Aroua *et al.* [14], where the B(GT) to the 2^+ state was scaled down by a factor of 3.

Negret et al., PRL 97 (2006)
KVI
RCNP

Magnetic moments of p-shell nuclei

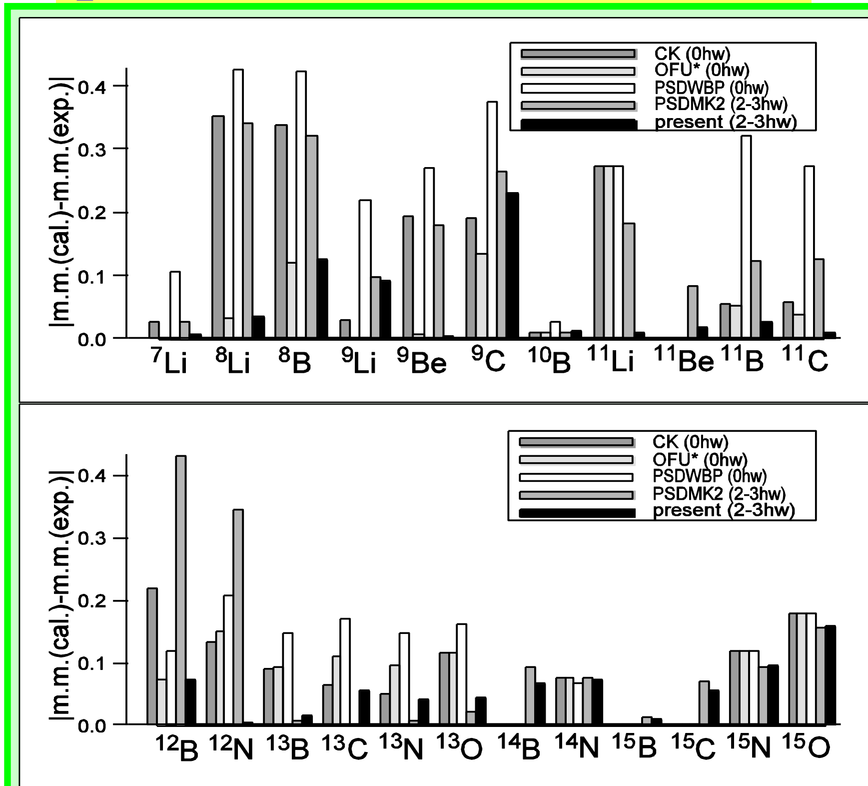

present = SFO **Suzuki, Fujimoto, Otsuka, PR C67 (2003)**

Space: up to 2-3 hw

SFO*: g_A^{eff}/g_A=0.95

B(GT: ^{12}C)_cal =experiment

Systematic improvements in the magnetic moments and GT transitions in p-shell nuclei (^{12}C, ^{14}C) .

SFO*: g_A^{eff}/g_A=0.95 (0 - 2, 3hw)
B(GT: 12C)_cal = experiment

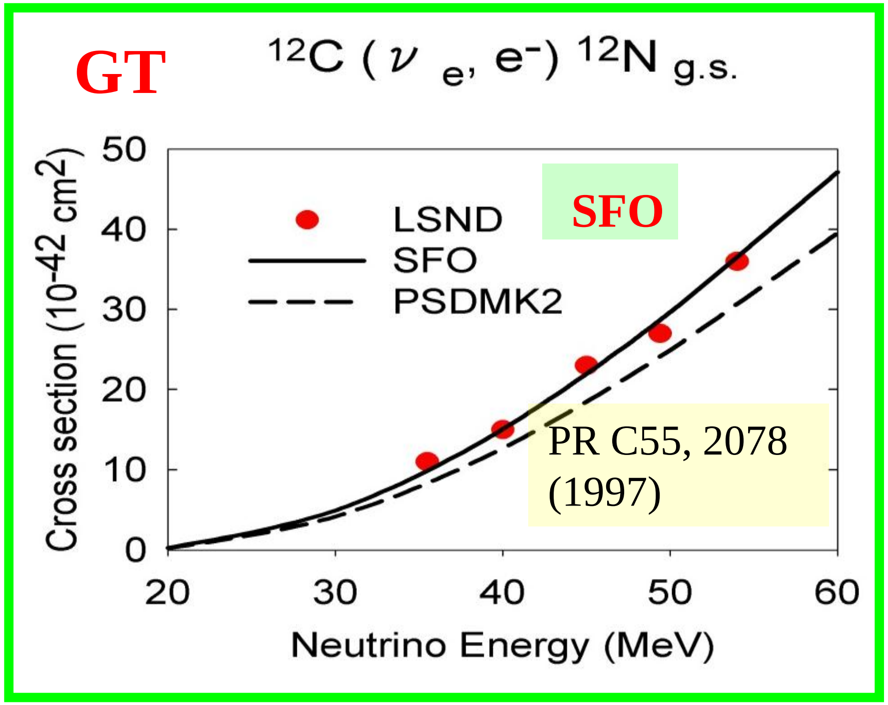

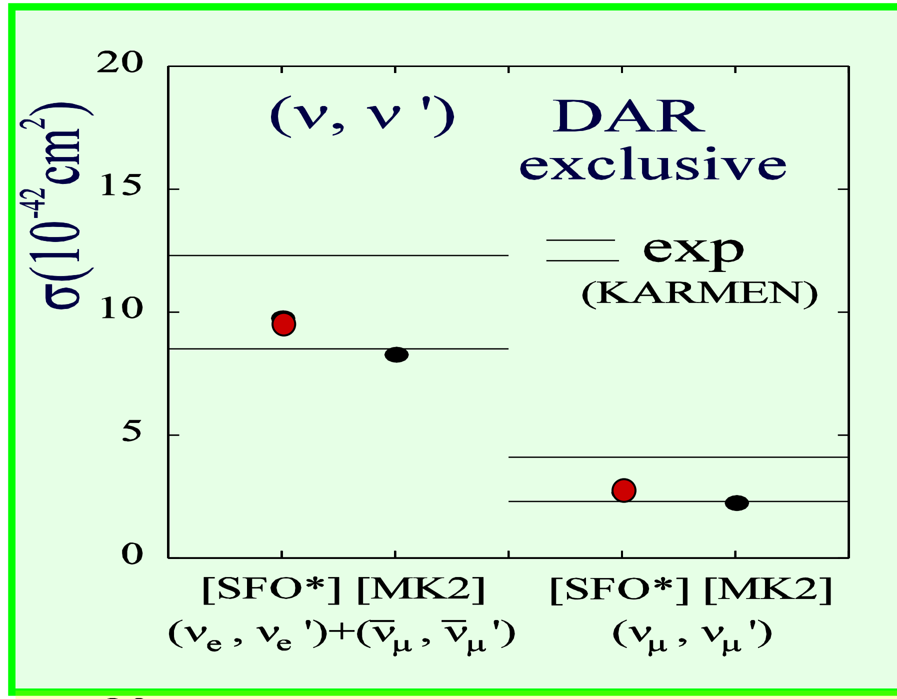

Suzuki, Chiba, Yoshida,Kajino, Otsuka, PR C74, 034307, (2006).

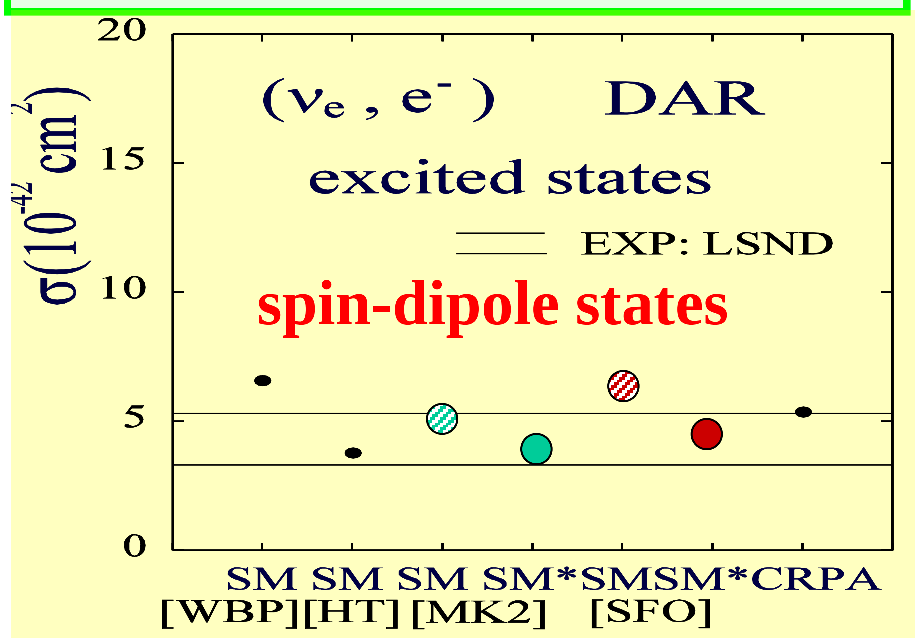

HT: Hayes-Towner, PR C62, 015501 (2000)
CRPA: Kolb-Langanke-Vogel, NP A652, 91 (1999)

Nucleosynthesis processes of light elements

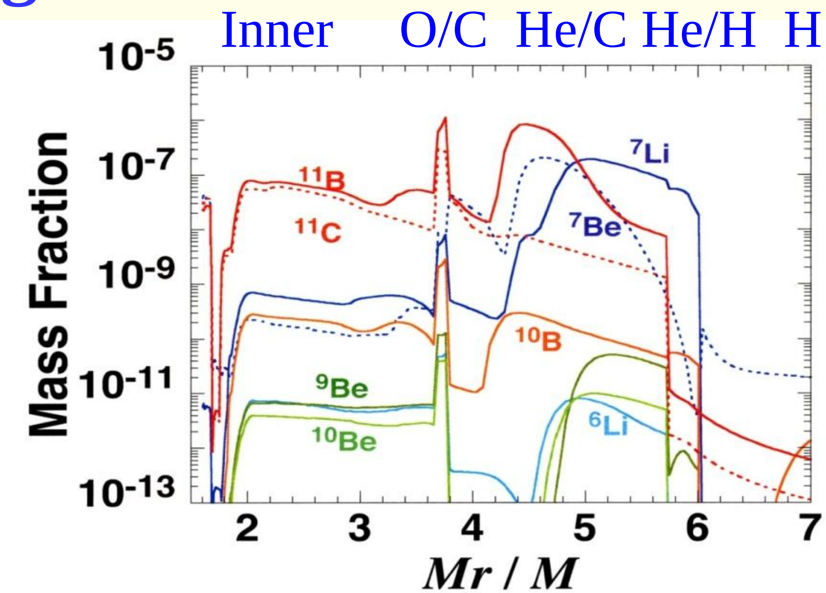

Fig. 4.— Mass fraction distribution of Model 1. The mass fractions of ^{7}Li and ^{7}Be, and ^{11}B and ^{11}C are separated.

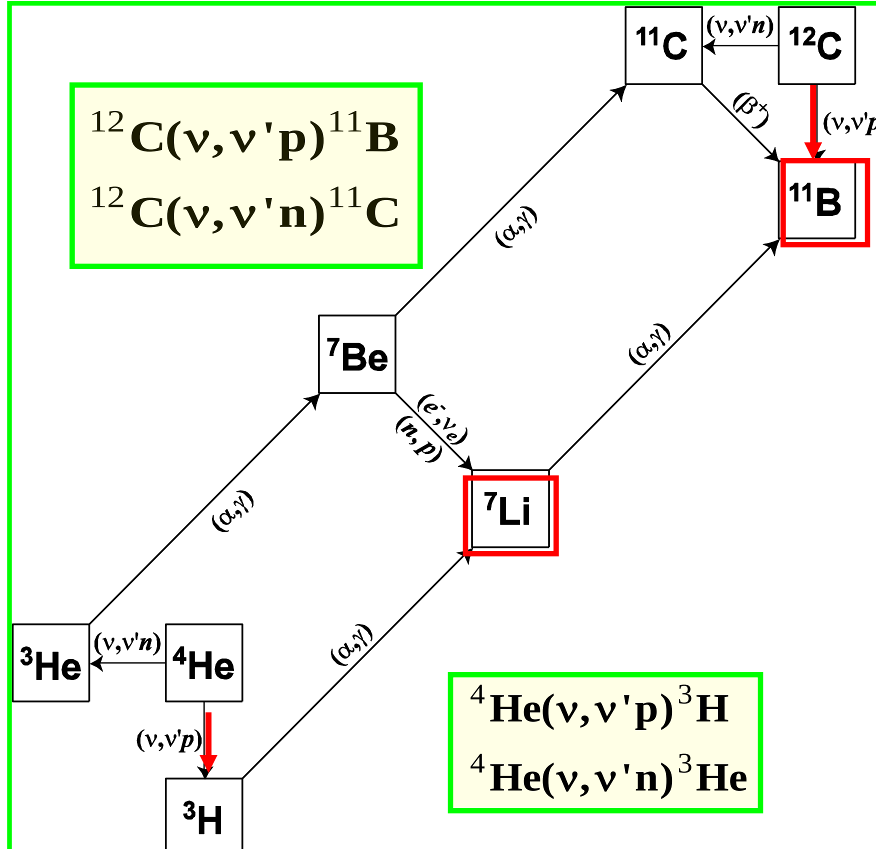

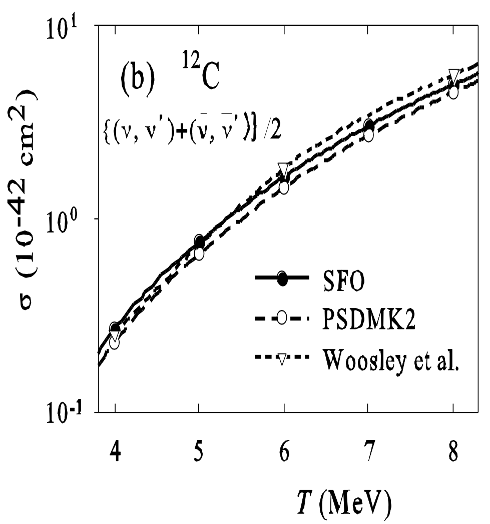

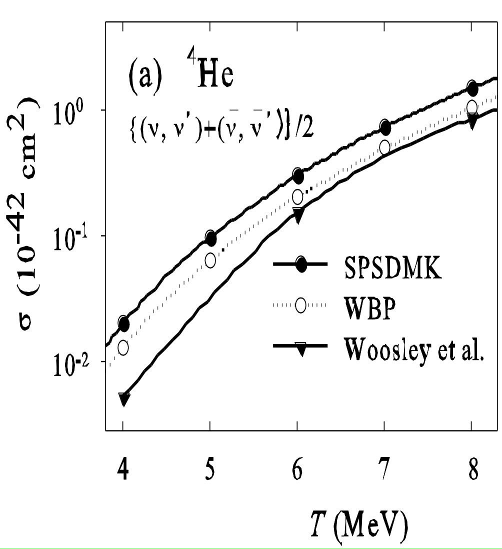

Enhancement of ^{11}B and ^{7}Li abundances in supernova explosions

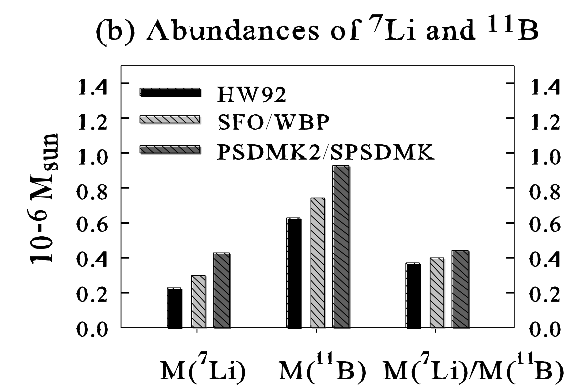

Normal hierarchy

Inverted hierarchy

ν oscillations

MSW effects

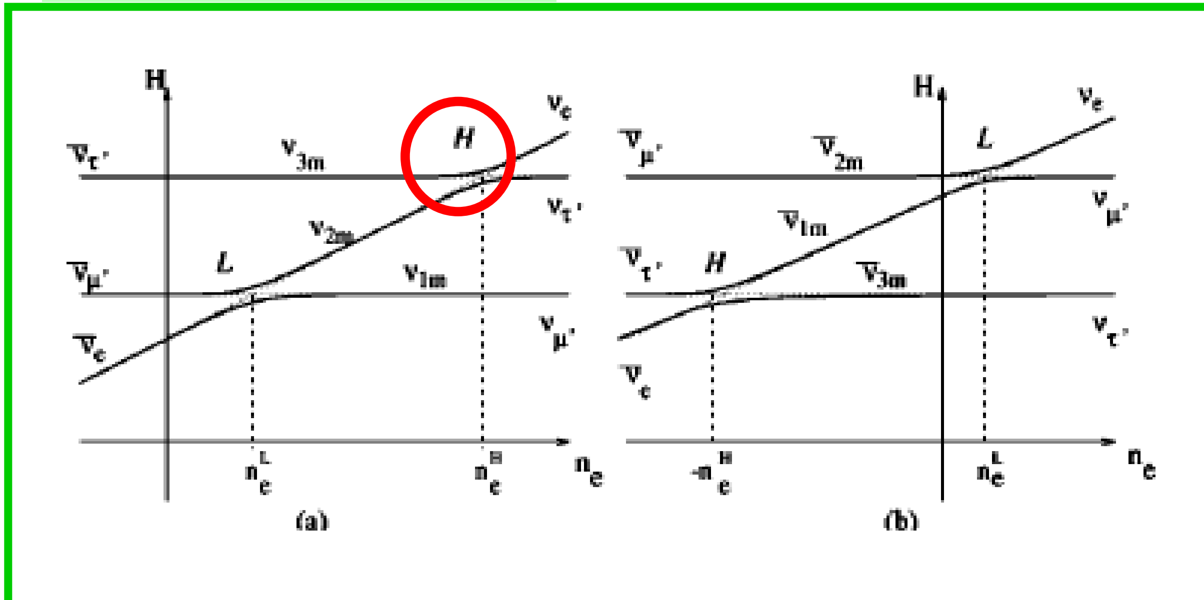

Normal – hierarchy

$$\nu_{\mu}, \nu_{\tau} \rightarrow \nu_{e}$$

Increase in the rates of charged-current reactions

4He$(\nu_e, e^- p)$**3He**

12C$(\nu_e, e^- p)$**11C**

in the He layer

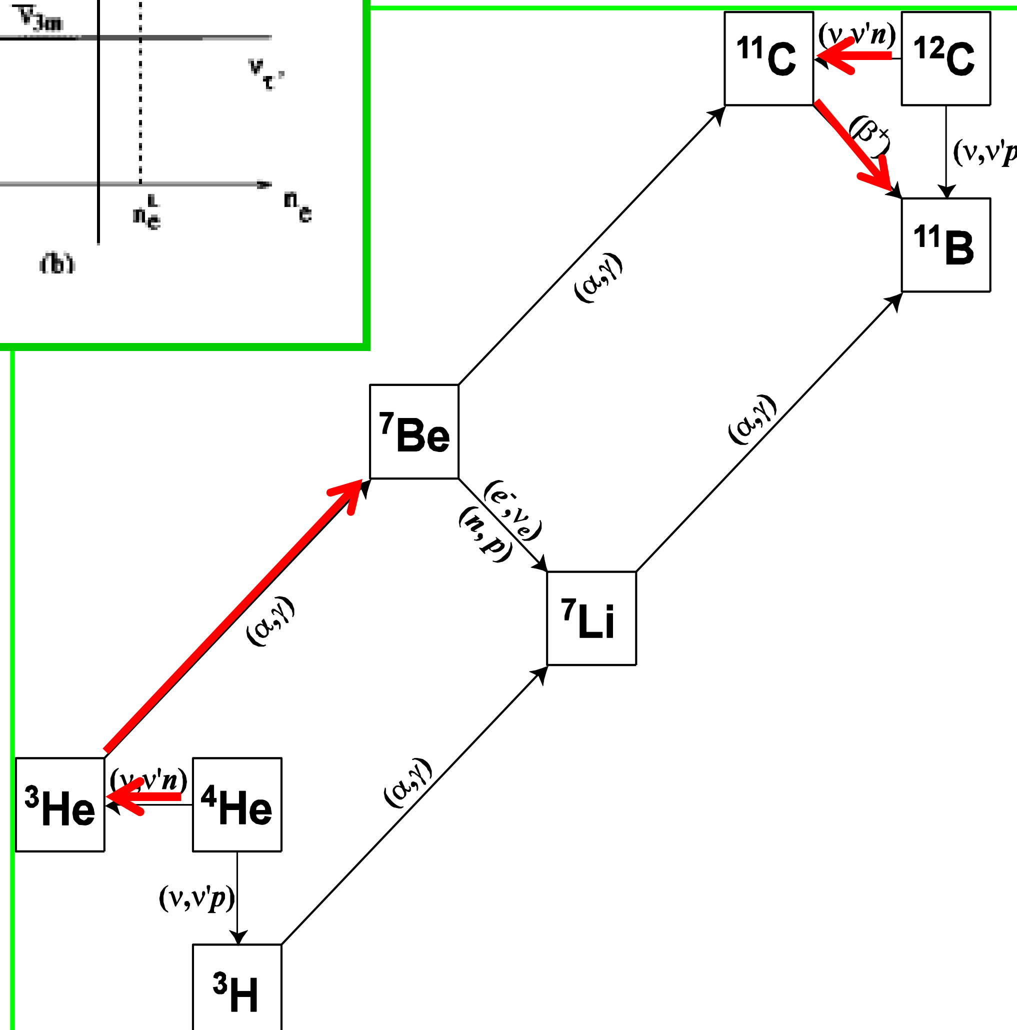

Supernova X-Grain Coinstraint

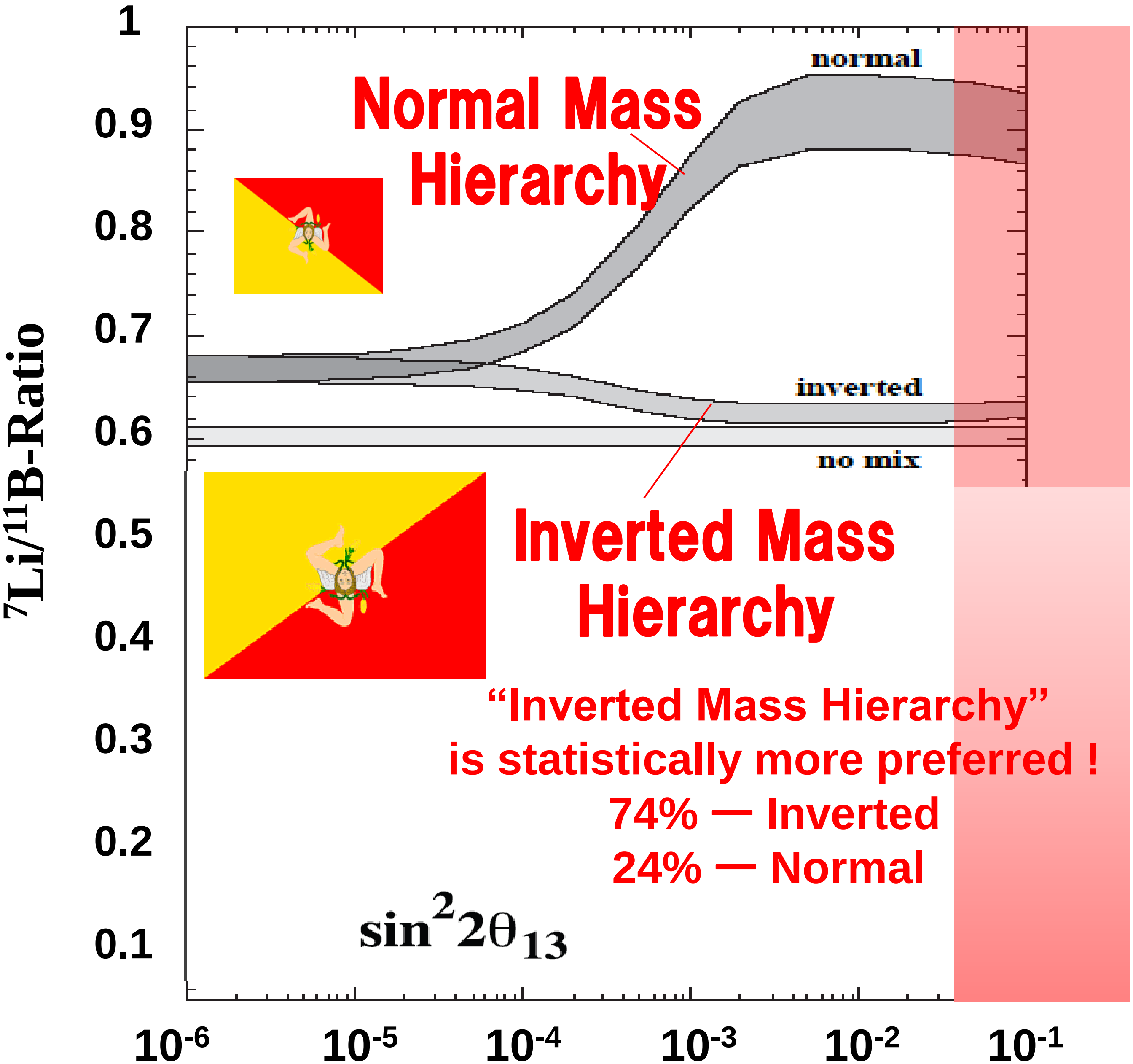

Mathews, Kajino, Aoki And Fujiya, Phys. Rev. D85,105023 (2012).

- T2K, MINOS (2011)
- Double CHOOZ, Daya Bay, RENO (2012)

$\sin^2 2\theta_{13} = 0.1$

First Detection of $^7Li/^{11}B$ in SN-grains

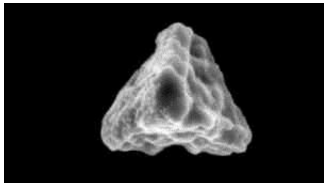

W. Fujiya, P. Hoppe, & U. Ott, ApJ 730, L7 (2011).

- New ν-^{13}C cross sections with SFO

  ^{13}C is a good target for low-energy ν detection; E<10 MeV

  Suzuki, Balantekin and Kajino, PR C86, 015502 (2012)

  $E_{th}(^{12}C) = 13$ MeV

  ^{13}C: 1% natural abundance in C isotopes

- New ν-^{16}O cross sections with SFO-tls

  Full inclusion of tensor force in p-sd cross shells:

  tensor → π+ρ   LS → σ+ρ+ω

$$\frac{\sigma(^{16}O(\nu,\nu'\alpha p)^{11}B)}{\sigma(^{12}C(\nu,\nu' p)^{11}B)} \approx 20\%$$

^{11}B is produced from ^{16}O also

▪ ν- ^{40}Ar reactions

Liquid argon = powerful target for SNν detection

VMU= Monopole-based universal interaction

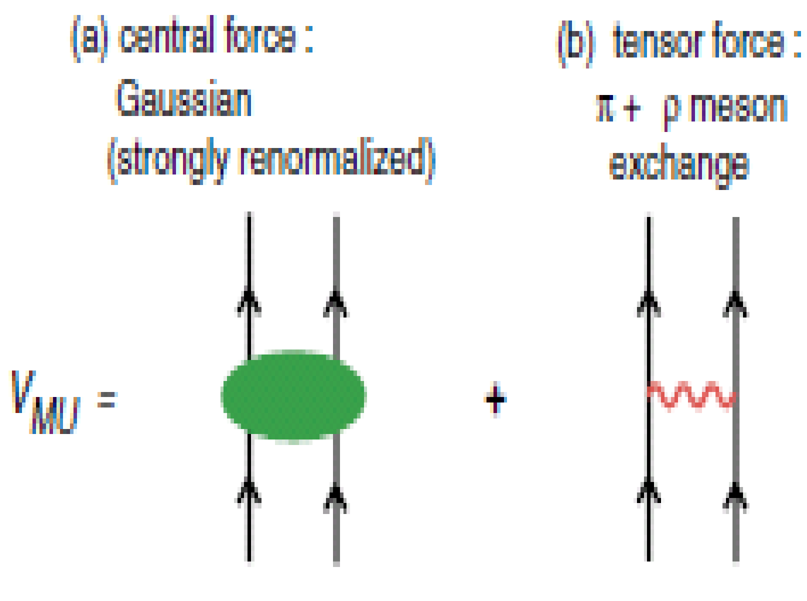

FIG. 2 (color online). Diagrams for the V_{MU} interaction.

Important roles of tensor force

Otsuka, Suzuki, Honma, Utsuno, Tsunoda, Tsukiyama, Hjorth-Jensen PRL 104 (2010) 012501

tensor force: bare≈renormalized

○ sd-pf shell: **^{40}Ar (ν, e$^-$) ^{40}K**

SDPF-VMU-LS

sd: SDPF-M (Utsuno et al.)

fp: GXPF1 (Honma et al.)

sd-pf: VMU + 2-body LS

$(sd)^{-2}$ $(fp)^2$: 2hw

B(GT) & ν-^{40}Ar cross sections

Solar ν cross sections folded over ^{8}B ν spectrum

Suzuki and Honma, PR C87, 014607 (2013)

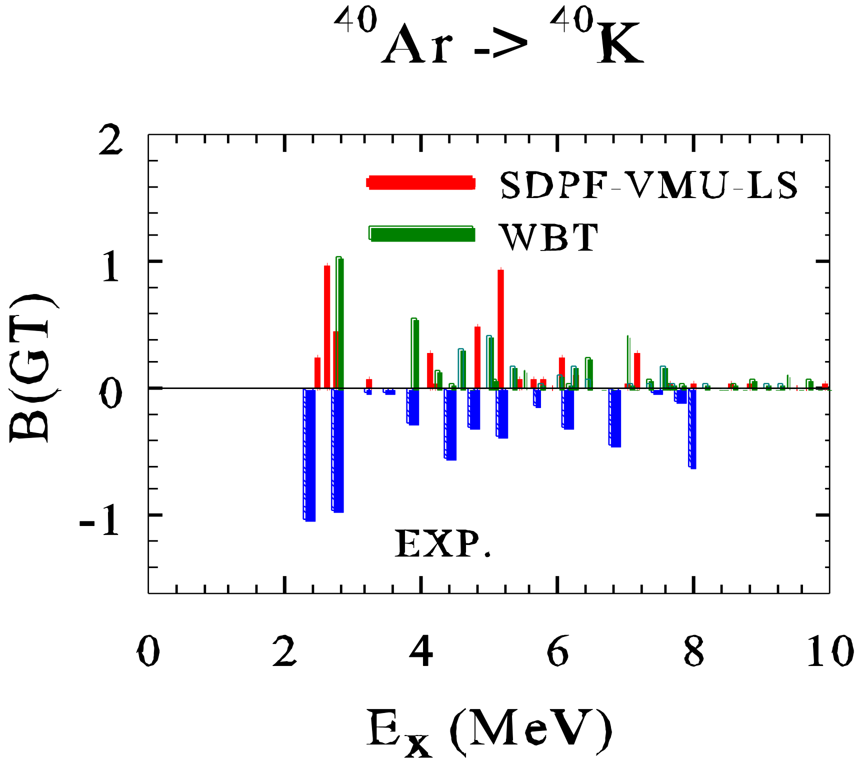

(p,n) Bhattacharya et al., PR C80 (2009)

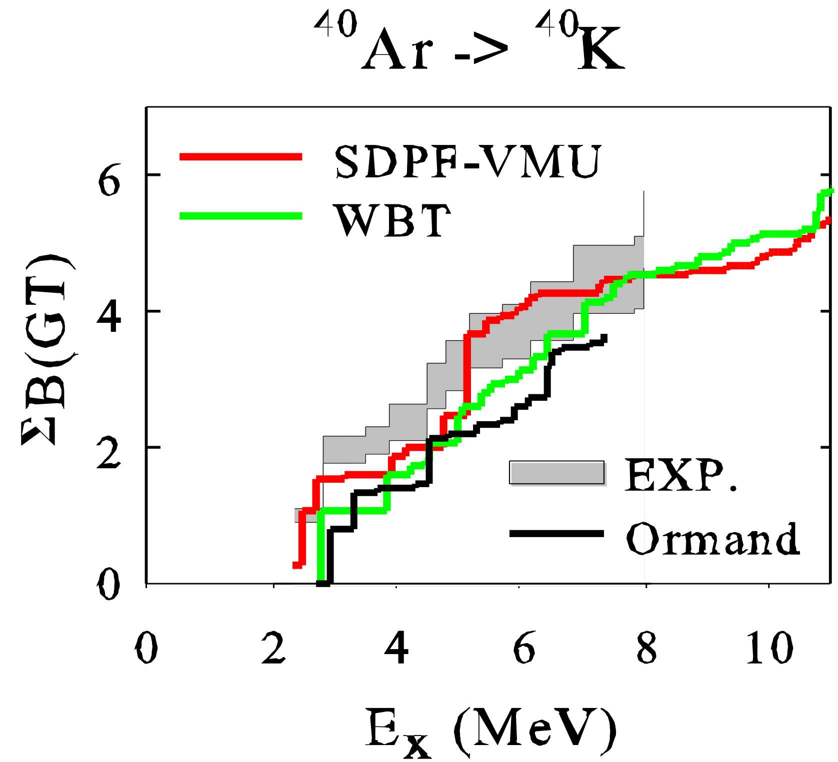

^{40}Ar (ν, e^-) ^{40}K
GT+IAS
E_e > 5 MeV : ICARUS

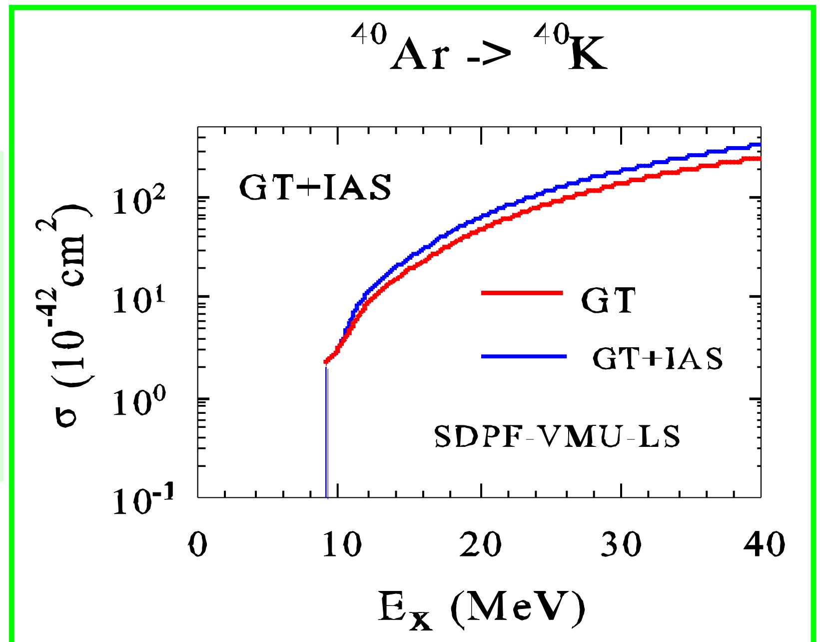

Solar ν cross sections folded over ^{8}B ν spectrum

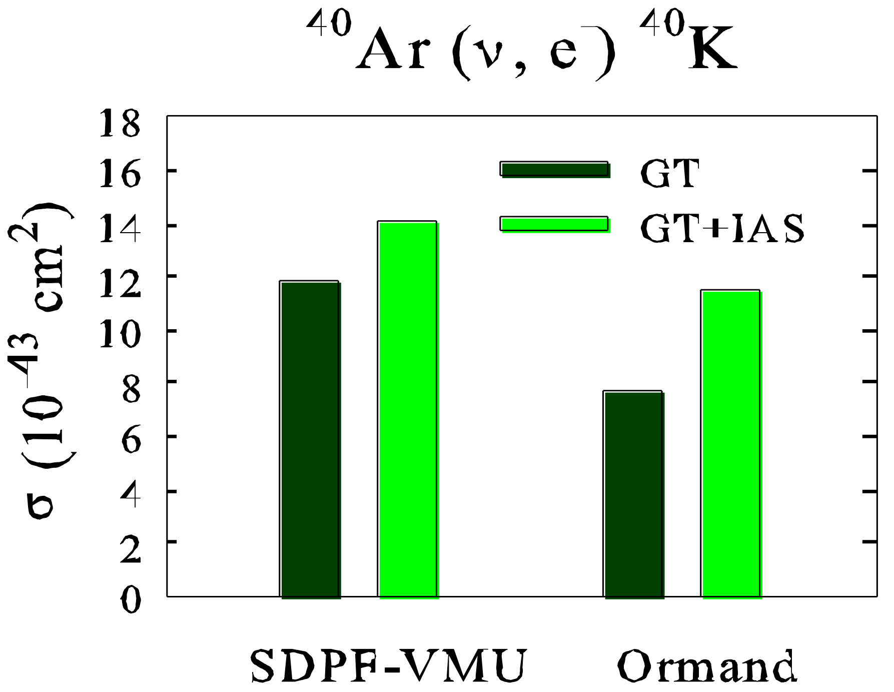

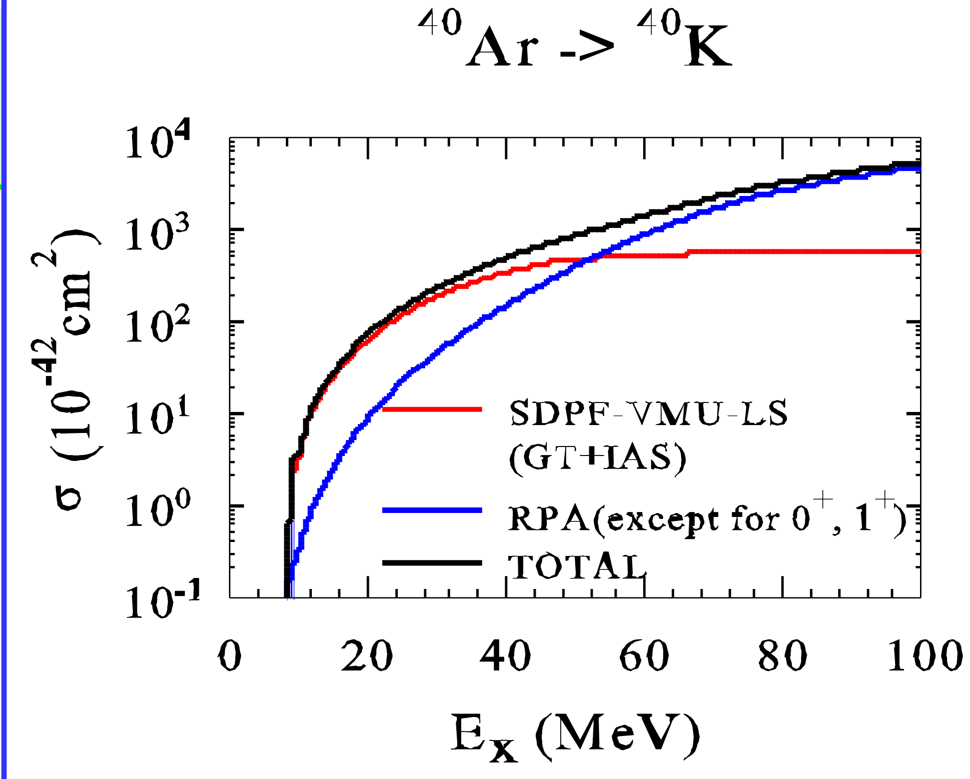

IAS: $C0+L0 \approx [(q^2-\omega^2)/q^2]^2 \times C0$; $^{+}$ C0 only

GT: $E_1^5 + M1 + C_1^5 + L_1^5$; $^{+}$ E_1^5 only

$^{+}$Ormand et al, PL B345, 343 (1995)

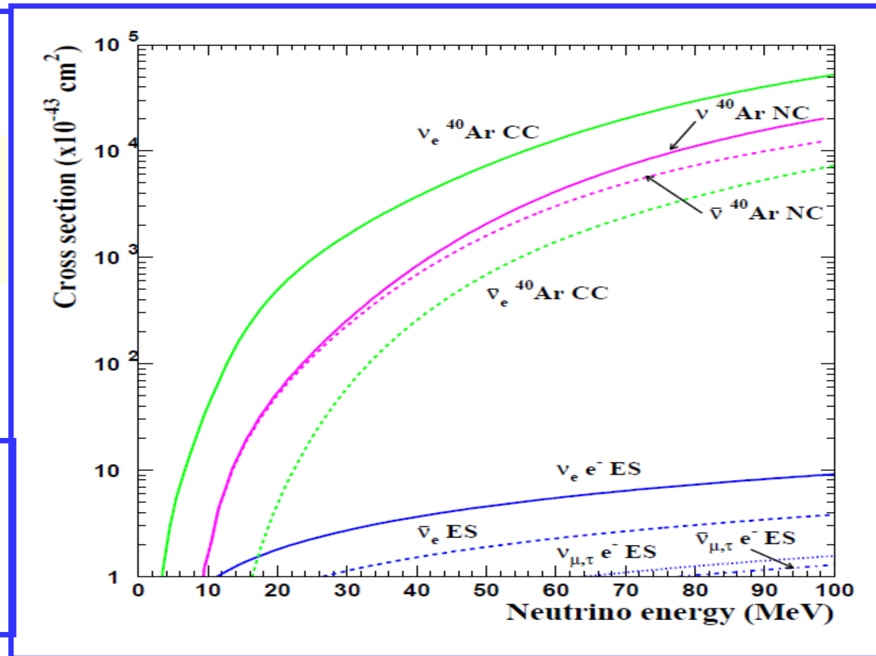

E. Kolbe, K. Langanke, G. Mart´ınez-Pinedo, and P. Vogel, J. Phys. G **29**, 2569 (2003);
I. Gil-Botella and A. Rubbia, JCAP **10**, 9 (2003).

○ p-sd shell: VMU for p-sd,

Yuan, Suzuki, Otsuka, Xu, Tsunoda,
PR C85, 064324 (2012) .

p: SFO sd: SDPF-M (Utsuno)

p-sd: VMU tensor = π+ρ,
2-body LS = σ+ρ+ω (M3Y)
central= renormalized VMU

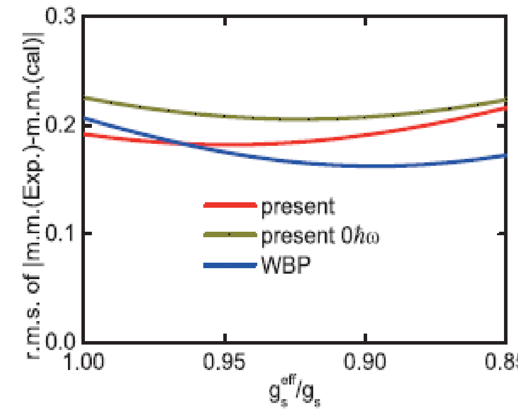

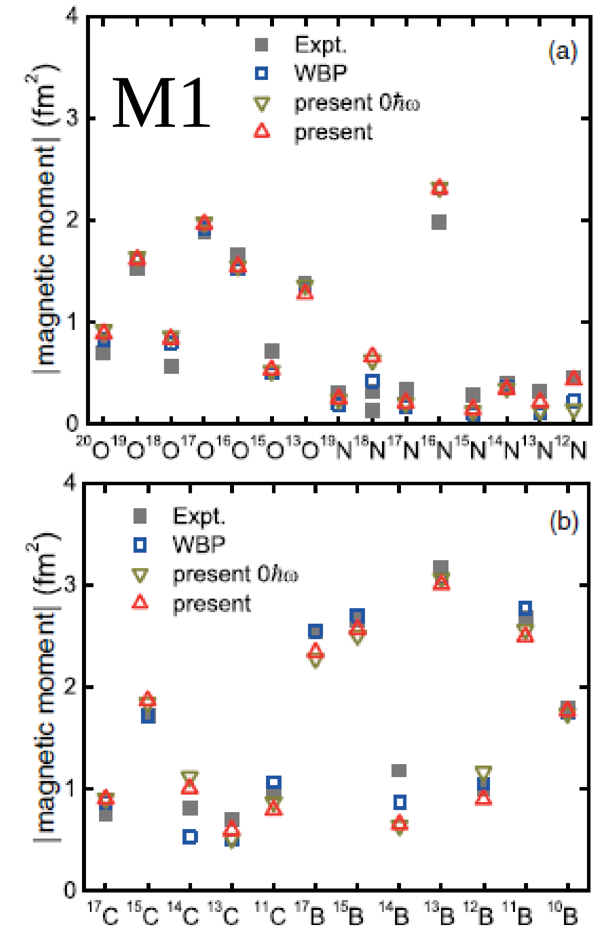

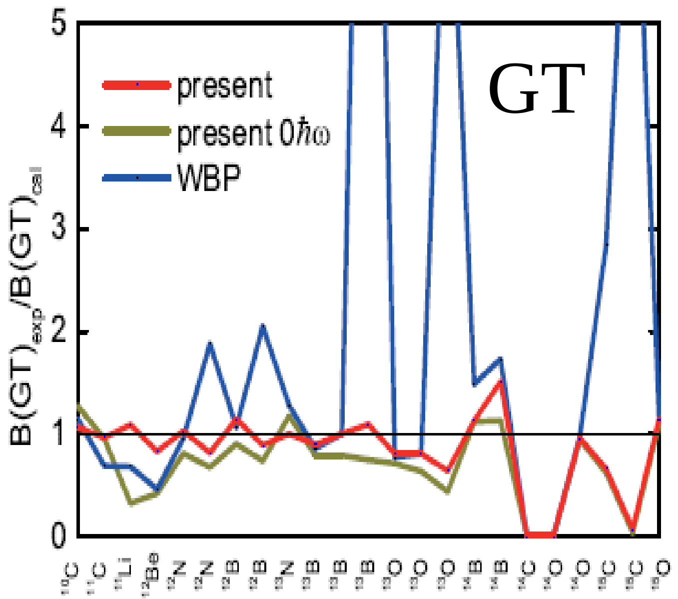

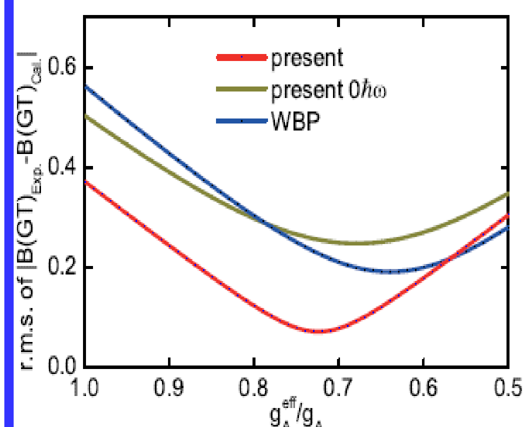

▪ ν- ^{56}Fe, ν- ^{56}Ni and ^{56}Ni (e$^-$, ν) ^{56}Co Reactions

New shell-model Hamiltonains in pf-shell

GXPF1: Honma, Otsuka, Mizusaki, Brown, PR C65 (2002); C69 (2004)

KB3: Caurier et al, Rev. Mod. Phys. 77, 427 (2005)

- ○ KB3G A = 47-52 KB + monopole corrections
- ○ GXPF1 A = 47-66

▪ **Spin properties of fp-shell nuclei are well described**

B(GT$_-$) for ^{58}Ni

$g_A^{eff}/g_A^{free}=0.74$

^{56}Fe → ^{56}Co

B(GT)=9.5
$B(GT)_{exp}=9.9 \pm 2.4$
$B(GT)_{KB3G}=9.0$

SD + … : RPA (SGII)

Fujita et al.

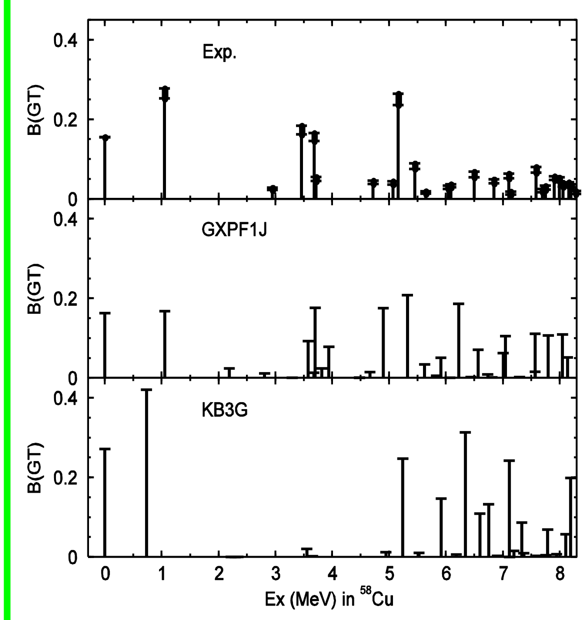

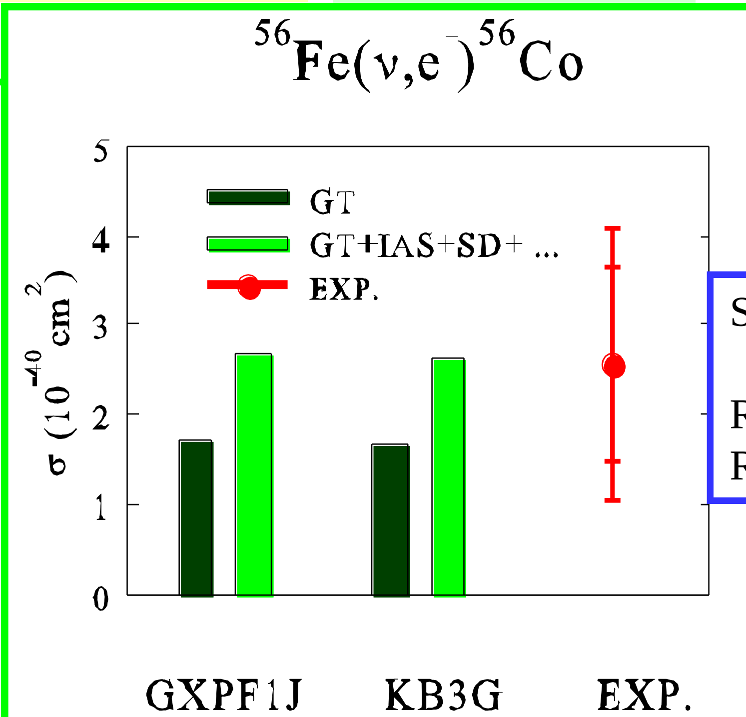

SM(GXPF1J)+RPA(SGII)
259 x10^{-42}cm^2
RHB+RQRPA(DD-ME2) 263
RPA(Landau-Migdal force) 240

$$\langle\sigma\rangle_{exp} = (256 \pm 108 \pm 43) \times 10^{-42}\ \mathrm{cm}^2.$$
$$\langle\sigma\rangle_{th} = (258 \pm 57) \times 10^{-42}\ \mathrm{cm}^2.$$

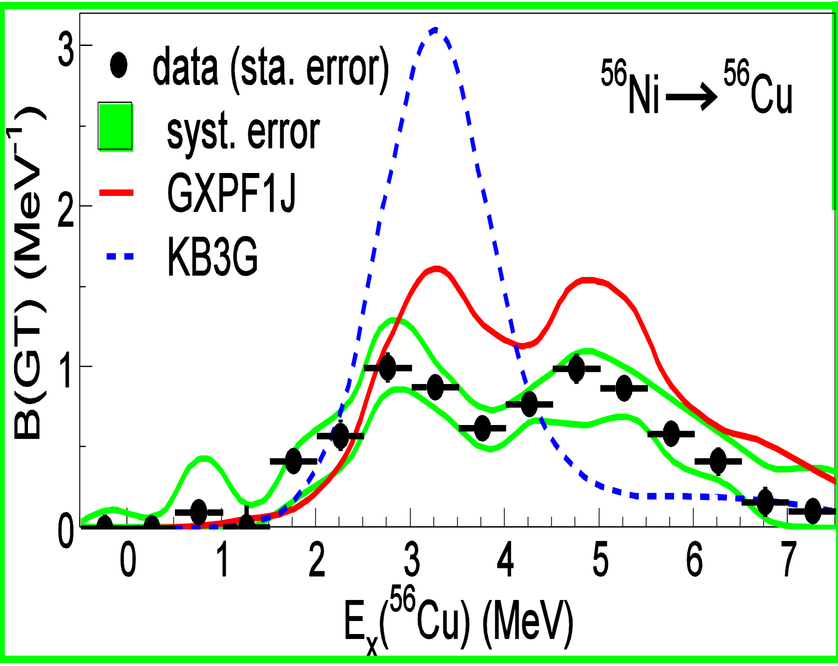

e-capture rates on ^{56}Ni in stellar environments: $\rho Y_e = 10^7 - 10^{10}$ g/cm^3

Sasano et al., PRL 107, 202501 (2011)

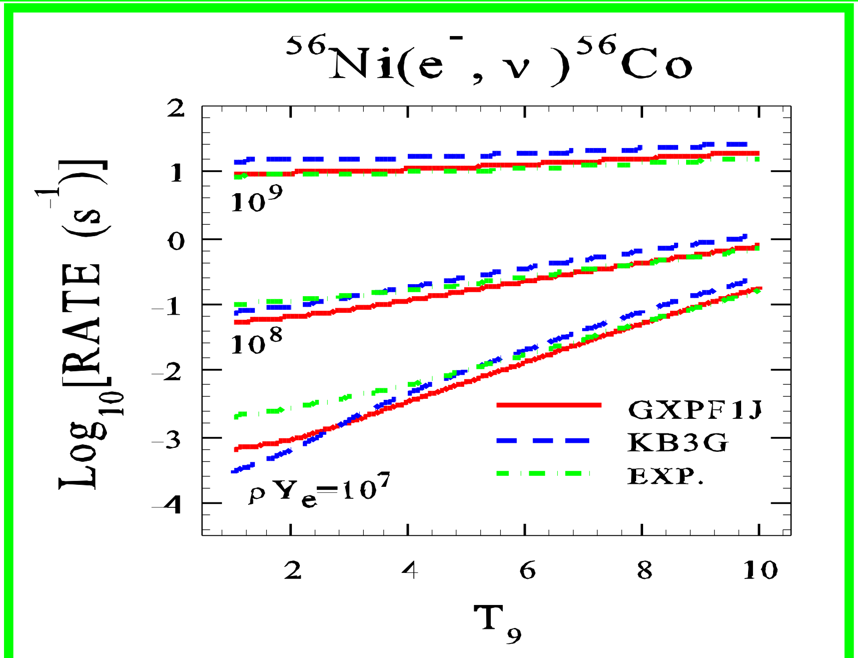

Suzuki, Honma, Mao, Otsuka, Kajino, PR C83, 044619 (2011)

Type-Ia supernova explosion

Accretion of matter to white-dwarf from binary star
→ supernova explosion when white-dwarf mass > Chandrasekhar limit
→ ^{56}Ni (N=Z)
→ ^{56}Ni (e$^-$, ν) ^{56}Co Y_e =0.5 → Y_e < 0.5 (neutron-rich)
→ production of neutron-rich isotopes; more ^{58}Ni
Decrease of e-capture rate on ^{56}Ni
→ less production of ^{58}Ni.

e-capture rates:
GXPF1J < KB3G
←→
Y_e (GXPF1J) > Y_e (KB3G)

Problem of over-production of ^{58}Ni may be solved.

Problem of over-production of ^{58}Ni

THE ASTROPHYSICAL JOURNAL SUPPLEMENT SERIES, 125:439–462, December

NUCLEOSYNTHESIS IN CHANDRASEKHAR MASS MODELS FOR TYPE Ia SUPERNOVAE AND CONSTRAINTS ON PROGENITOR SYSTEMS AND BURNING-FRONT PROPAGATION

KOICHI IWAMOTO,[1,2,3] FRANZISKA BRACHWITZ,[4] KEN'ICHI NOMOTO,[1,2,3] NOBUHIRO KISHIMOTO,[1]
HIDEYUKI UMEDA,[2,3] W. RAPHAEL HIX,[3,5] AND FRIEDRICH-KARL THIELEMANN[3,4,5]

Received 1999 January 11; accepted 1999 July 29

and ignition densities to put new constraints on the above key quantities. The abundance of the Fe group, in particular of neutron-rich species like ^{48}Ca, ^{50}Ti, ^{54}Cr, ^{54,58}Fe, and ^{58}Ni, is highly sensitive to the electron captures taking place in the central layers. The yields obtained from such a slow central

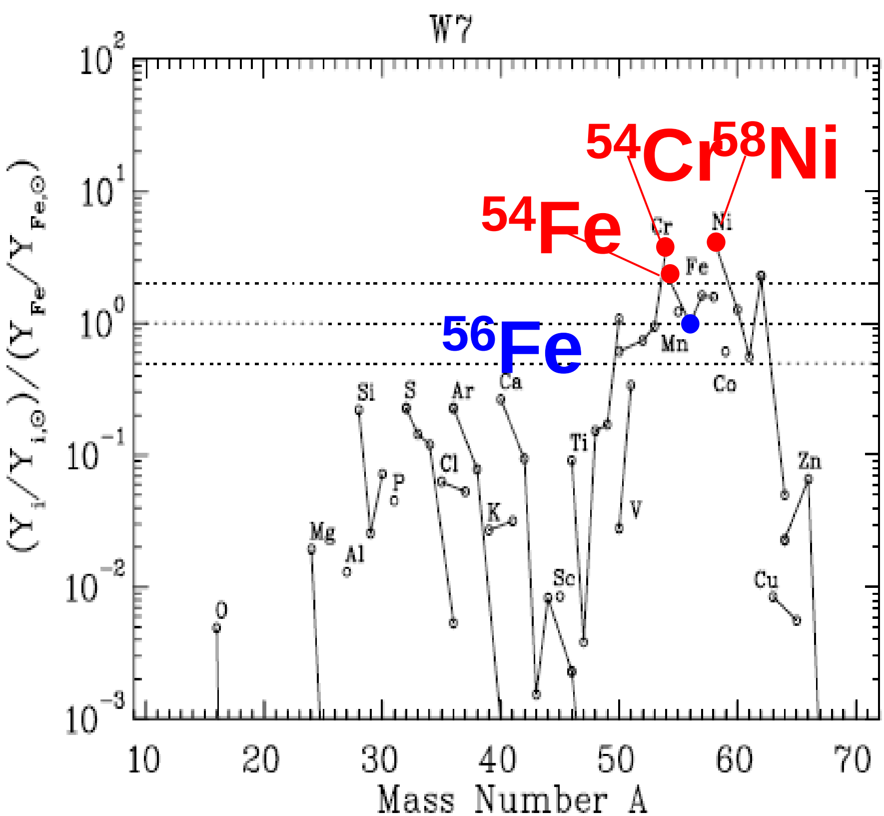

Famiano

NSE(Nuclear Statistical Equilibrium) calculation

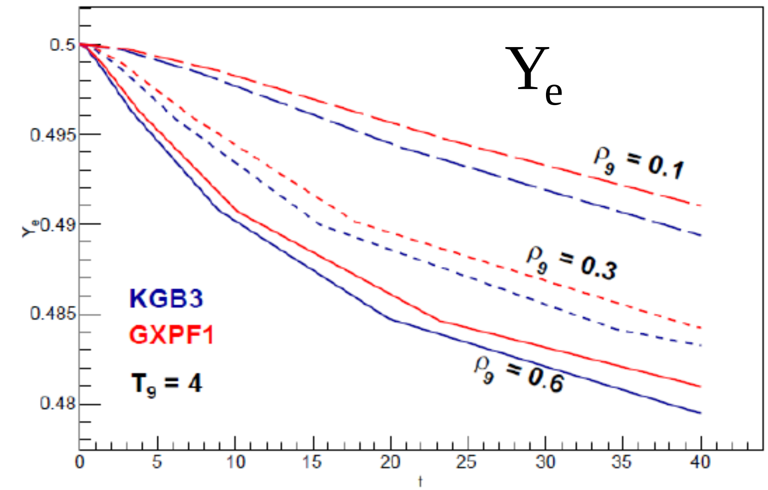

Ratio between ^{58}Ni / ^{56}Ni

GXPF1 -> ^{58}Ni/^{56}Ni decreases

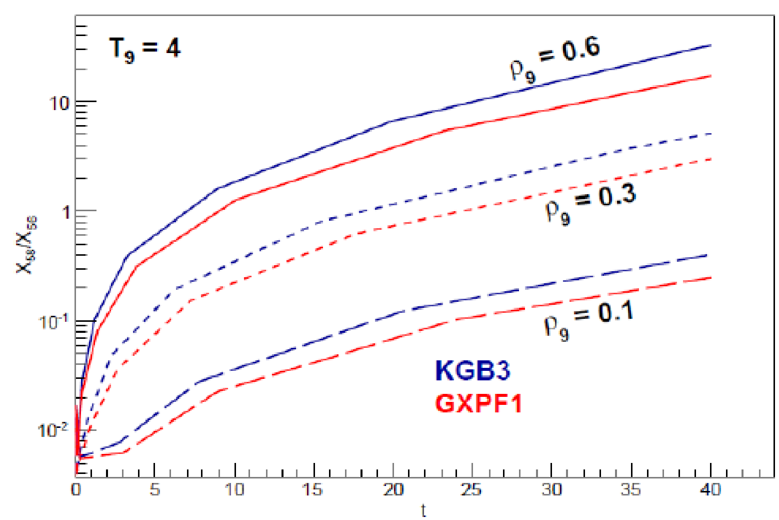

○Evolution of 8-10M$_\odot$ stars and nuclear URCA processes

- M=0.5 ～8M$_\odot$

  He burning → C-O core → C-O white dwarfs

- M >10M$_\odot$

  → Fe core → core-collapse supernova explosion

- M=8M$_\odot$ ～ 10M$_\odot$

  C burning → O-Ne-Mg core

  → (1) O-Ne-Mg white dwarf (WD)

  → (2) e-capture supernova explosion (collapse of O-Ne-Mg core induced by e-capture) with neutron star (NS) remnant

  → (3) core-collapse (iron-core collapse) supernova explosion with NS (neon burning shell propagates to the center)

Fate of the star is sensitive to its mass and nuclear e-capture and β–decay rates; Cooling of O-Ne-Mg core by nuclear URCA processes determines (2) or (3).

Nomoto and Hashimoto, Phys. Rep. 163, 13 (1988)
Miyaji, Nomoto, Yokoi, and Sugimoto, Pub. Astron. Soc. Jpn. 32, 303 (1980)
Nomoto, Astrophys. J. 277, 791 (1984); ibid. 322, 206 (1987)

▪ Detailed e-capture and beta-decay rates for URCA nuclear pairs in 8-10 solar-mass stars

Nuclear URCA process

$$^{23}Na + e^- \rightarrow ^{23}Ne + \nu$$

$$^{23}Ne \rightarrow ^{23}Na + e^- + \bar{\nu}$$

$$^{25}Mg + e^- \rightarrow ^{25}Na + \nu$$

$$^{25}Na \rightarrow ^{25}Mg + e^- + \bar{\nu}$$

$$^{27}Al + e^- \rightarrow ^{27}Mg + \nu$$

$$^{27}Mg \rightarrow ^{27}Al + e^- + \bar{\nu}$$

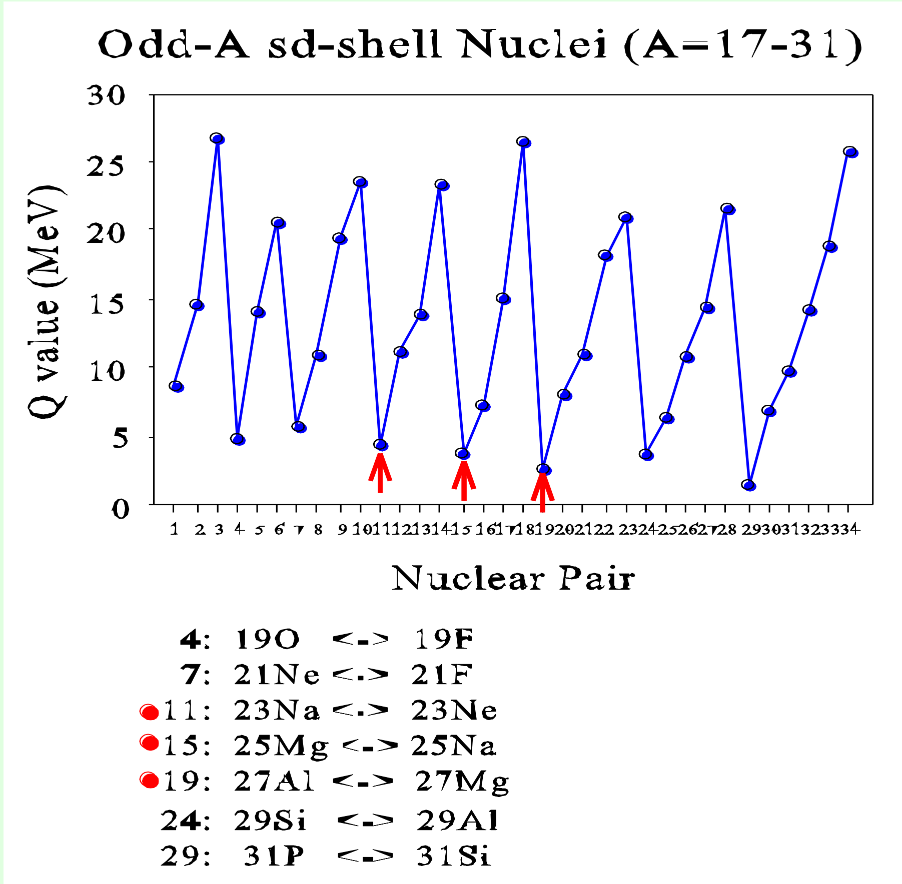

Cooling of O-Ne-Mg core of stars

→ ‘e-cap.SNe’ or ‘core-collapse SNe’

sd-shell: USDB Brown and Richter, PR C74, 034315 (2006)

Richter, Mkhize, Brown, PR C78, 064302 (2008)

(^{23}Ne, ^{23}Na)

PHYSICAL REVIEW C 88, 015806 (2013)

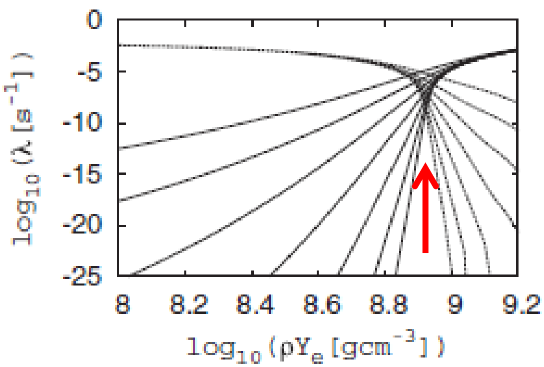

FIG. 2. β-transition rates for the $A = 23$ URCA nuclear pair (^{23}Ne, ^{23}Na) for various temperatures as functions of density $\log_{10} \rho Y_e$. β-decay rates (dashed lines) are those decreasing with density, while electron-capture rates (solid lines) are those increasing with density. The temperature steps are shown in the range of $\log_{10} T = 8$ to 9.2 in steps of 0.2.

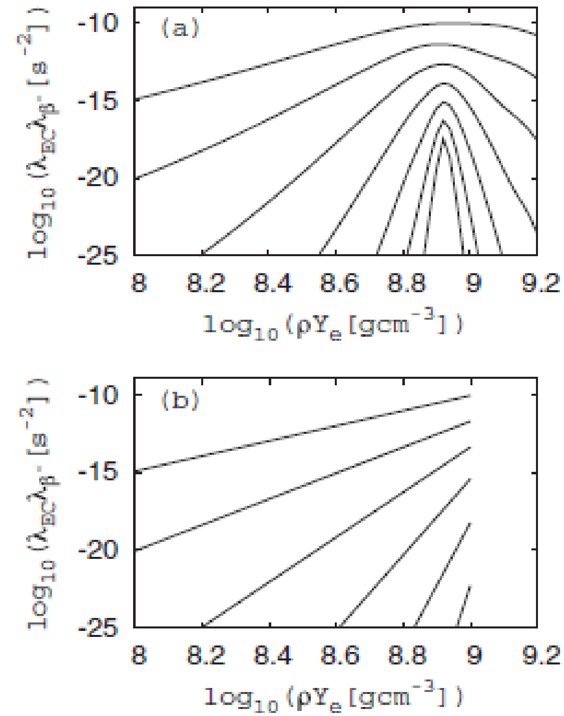

FIG. 3. Product of β-transition rates for the $A = 23$ URCA nuclear pair (^{23}Ne, ^{23}Na) for various temperatures as functions of density $\log_{10} \rho Y_e$. In panel (a), the mesh points are taken from $\log_{10} \rho Y_e = 8.0$ to 9.2 in steps of 0.02, while in panel (b), they are from $\log_{10} \rho Y_e = 8.0$ to 9.0 in a single step as in Oda *et al.* [10].

$$\Delta \log_{10}(\rho Y_e) = 0.06$$

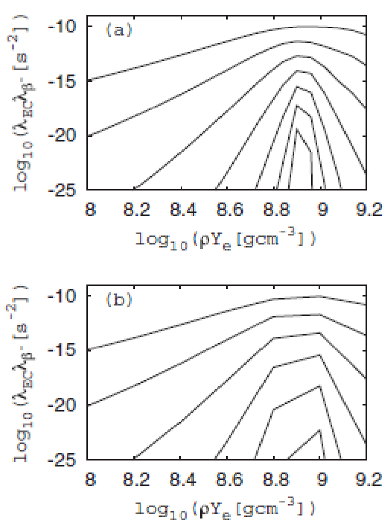

$$\Delta \log_{10}(\rho Y_e) = 0.2$$

$$8.0 < \log_{10}(\rho Y_e) < 9.2 \quad \text{in steps of } 0.02$$

$$8.0 < \log_{10} T < 9.2 \quad \text{in steps of } 0.05$$

cf: Oda et al., At. Data and Nucl. Data Tables 56, 231 (1994): $\Delta \log_{10}(\rho Y_e) = 1.0$

URCA density at $\log_{10} \rho Y_e = 8.92$ for $A = 23$

Cooling of O-Ne-Mg core by the nuclear URCA processes

(^{25}Na, ^{25}Mg)

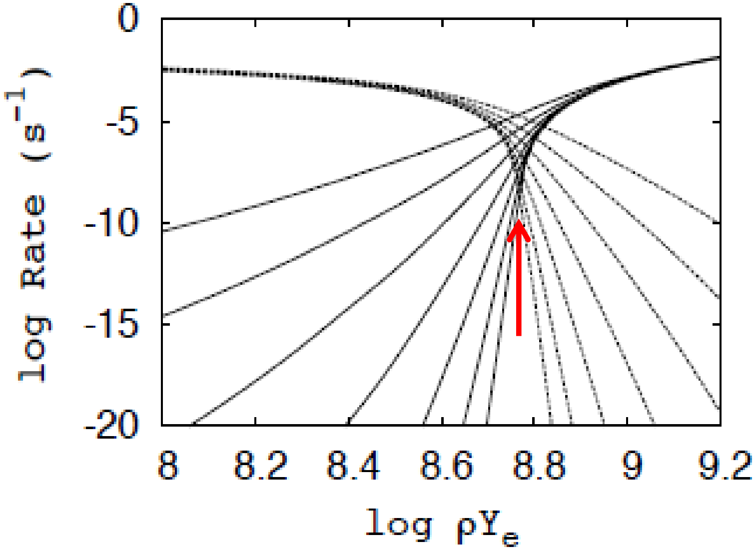

URCA density at $\log_{10} \rho Y_e = 8.78$

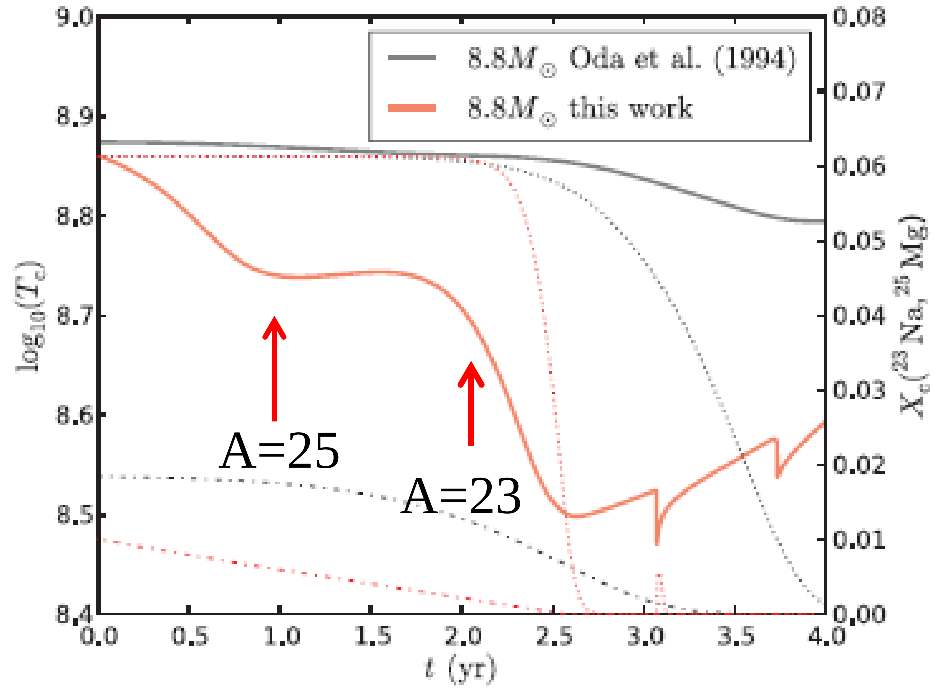

(^{27}Mg, ^{27}Al)

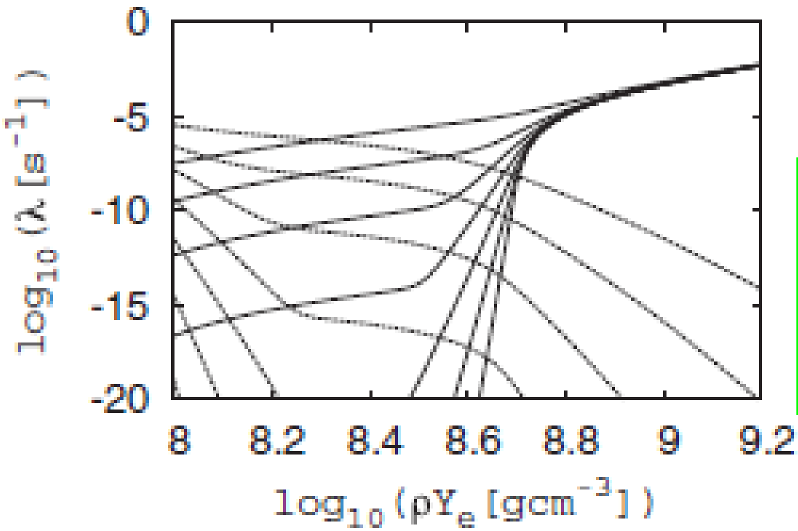

No clear URCA density for A=27

8.8$M_\odot$ star collapses triggered by subsequent e-capture on ^{24}Mg and ^{20}Ne (e-capture supernova explosion)

Toki, Suzuki, Nomoto, Jones and Hirschi, PR C 88, 015806 (2013)

Jones et al., Astrophys. J. 772, 150 (2013)

Table 1
Summary of Model Properties

	8.2 $M_\odot$	8.7 $M_\odot$	8.75 $M_\odot$	8.8 $M_\odot$	9.5 $M_\odot$	12.0 $M_\odot$
$M^{C}_{ign}/M_\odot$ [a]	0.15	0.00	0.00	0.00	0.00	0.00
$M^{Ne}_{ign}/M_\odot$ [b]	...	...	...	0.93	0.42	0.00
T^{Ne}_{ign}/GK [c]	...	...	...	1.318	1.311	1.324
ψ_c^{Ne} [d]	...	...	...	46.0	15.2	5.6
ρ_c^{Ne}/g cm^{-3} [e]	...	...	...	3.343×10^8	7.396×10^7	1.730×10^7
$M_{tot}/M_\odot$ [f]	7.299	7.910	8.572	8.544	9.189	11.338
$M_{env}/M_\odot$ [g]	6.031	6.559	7.210	7.174	6.702	8.023
$M_{He}/M_\odot$ [h]	1.26721	1.35092	1.36230	1.36967	2.48733	3.31580
$M_{CO}/M_\odot$ [i]	1.26695	1.35086	1.36227	1.36964	1.49246	1.88602
Remnant	ONe WD	ONe WD/NS	NS	NS	NS	NS
SN type	...	.../EC-SN (IIP)	EC-SN (IIP)	EC-SN (IIP)	CC-SN (IIP)	CC-SN (IIP)

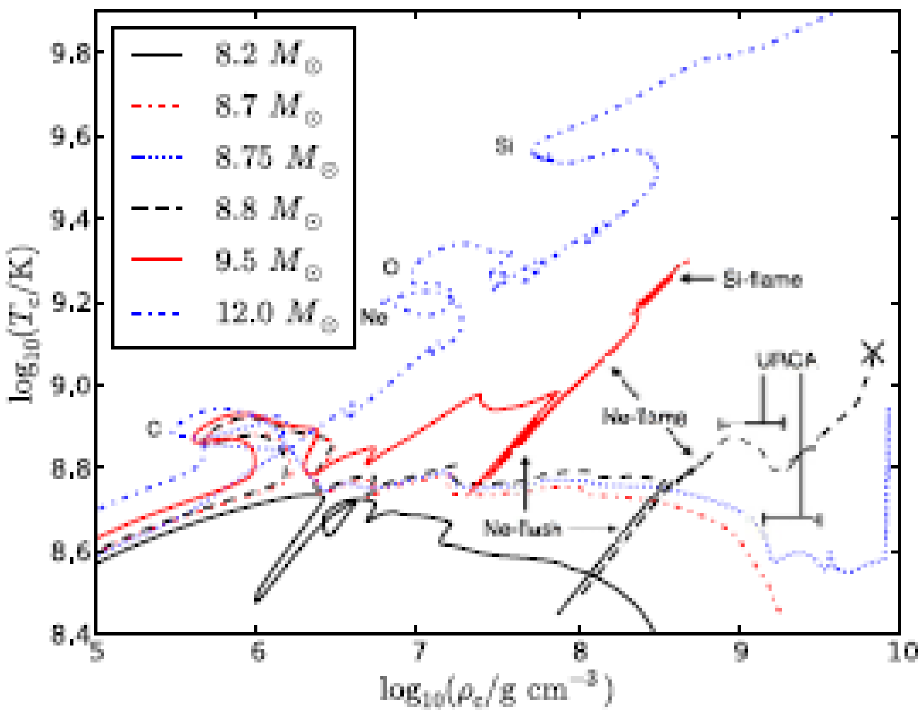

Jones et al., Astrophys. J. 772, 150 (2013)

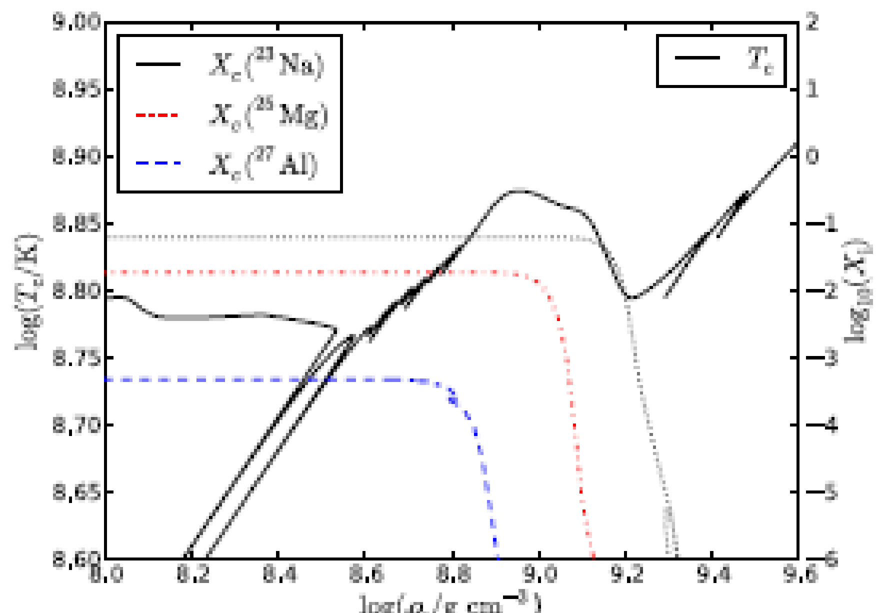

Coulomb corrections: screening effects

1. Screening effects of electrons

$$V(r) = -\frac{Ze^2}{2\pi^2}\int \frac{e^{i\vec{k}\vec{r}}}{k^2\epsilon(k,0)}d^3k = -\frac{Ze^2 2k_F}{2k_F r}\frac{2}{\pi}\int \frac{\sin(2k_F q r)}{q^2\epsilon(q,0)}dq.$$

$V(r)$ with screening effects of relativistic degenerate electron liquid

$$V_s(r) = V(r) - \left(-\frac{Ze^2}{r}\right) = Ze^2(2k_F)J,$$

Juodagalvis et al., Nucl. Phys. A 848, 454 (2010).
Itoh et al, Astrophys. J. 579, 380 (2002).

Vs(0)>0 → reduce both e-capture and β-decay rates

2. Change of threshold energy

$$\Delta Q_C = \mu_C(Z-1) - \mu_C(Z),$$

$\mu_C(Z)$ =the correction of the chemical potential of the ion with Z

ΔQ_c → reduce e-capture rates & enhance β-decay rates

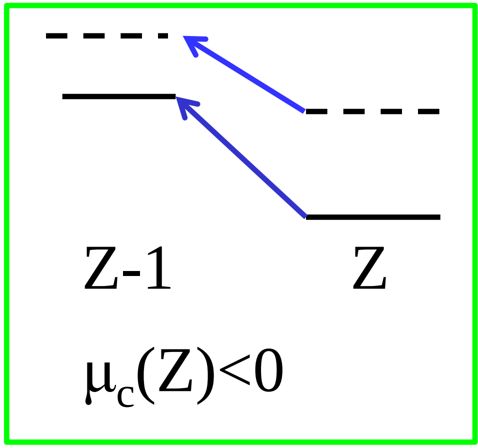

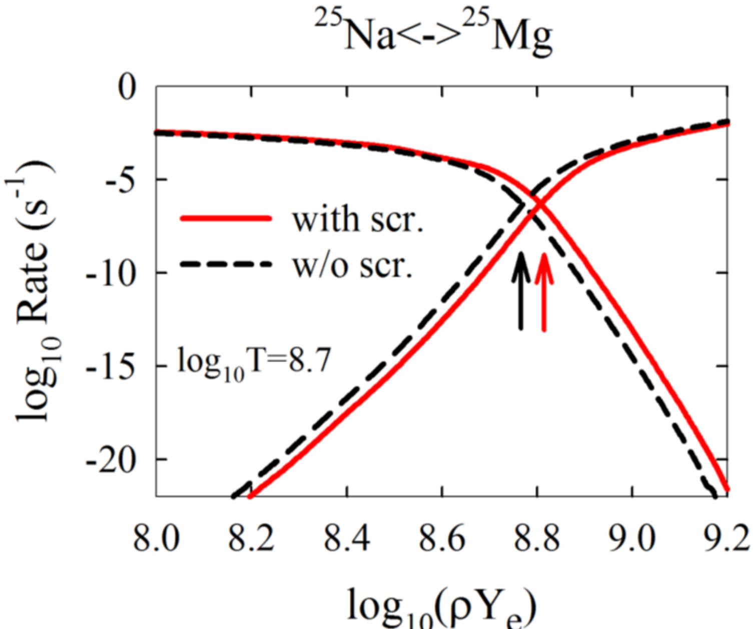

Slattery, Doolen, DeWitt, Phys. Rev. A26, 2255 (1982).
Ichimaru, Rev. Mod. Phys. 65, 255 (1993).

$$\rho Y_e = 8.78 \rightarrow 8.81$$

URCA density → higher density region

2. Structure of Ca (and O) isotopes and three-body forces

Shell model

G-matrix vs. G-matrix + three-body force

G = BonnC, CD-Bonn for Ca; 3rd-order Q-box

G = Kuo, BonnC, CD-Bonn for O

Hjorth-Jensen, Kuo, Osnes Phys. Rep. 261 (1995) 125.

FM (Fujita-Miyazawa) three-body force)

Δ-excitation by two-pion exchange

- Effective neutron single-particle energies
- Ground state energies
- E_x (2^+)
- M1 transition in ^{48}Ca

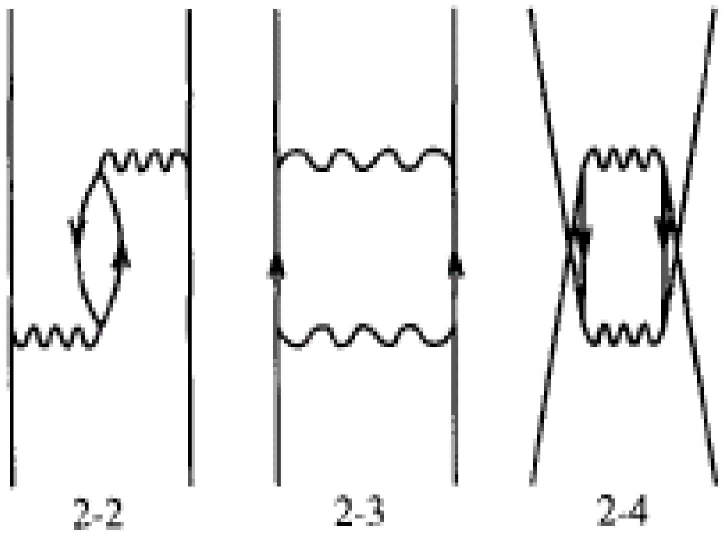

+3rd-order

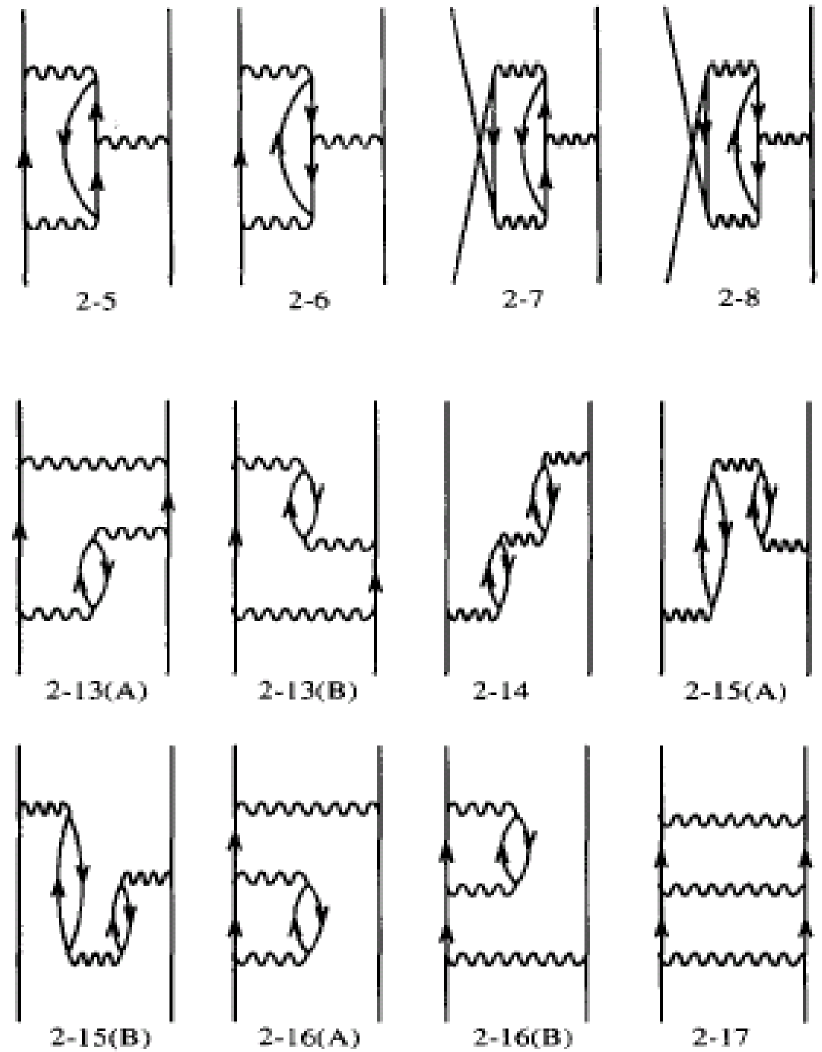

core-polarization effects

Kuo (HJ): 2nd-order, up to 2hw
BonnC: 3rd-order, up to 2-4 hw
CD-Bonn: 3rd-order, up to 24hw

etc.

Hjorth-Jensen et al., Phys. Rep. 261, 125 (1995)
T. T. S. Kuo, Nucl. Phys. A103, 71 (1967)

more repulsion than G in T=1
more attraction than G in T=0

- **Tensor force + repulsive corrections in T=1 monopoles**
  → SFO-tls
  - **Structure of neutron-rich C isotopes; exotic M1 transitions in ^{17}C is explained**
    (Suzuki-Otsuka, PR C78 (2008))

- **3 body forces induced by Δ excitations (Fujita-Miyazawa)**
  →repulsion in T=1monopoles
  →drip-line at ^{24}O in O isotopes
  (Otsuka, Suzuki, Holt, Schwenk, Akaishi, PRL 105, (2010))

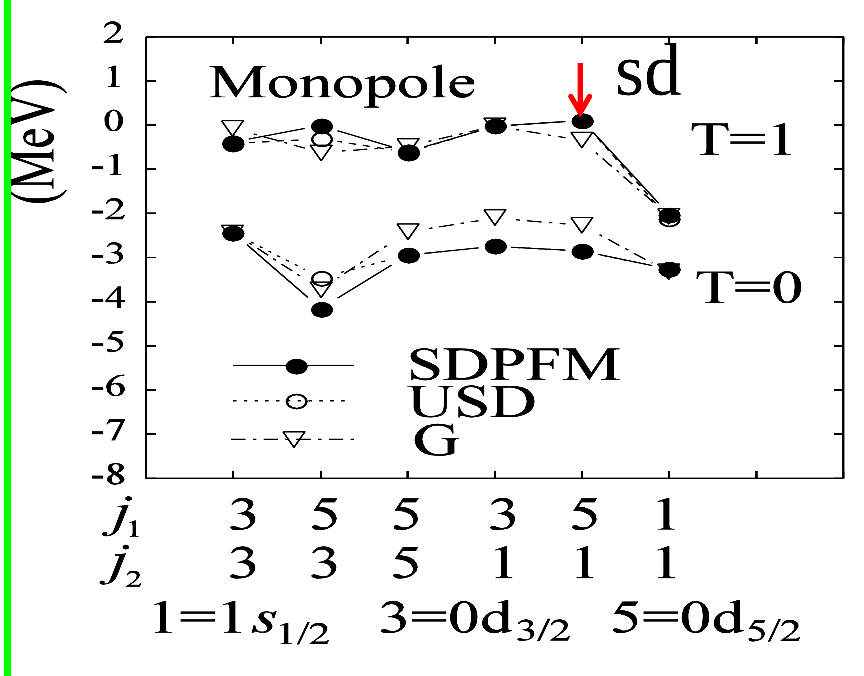

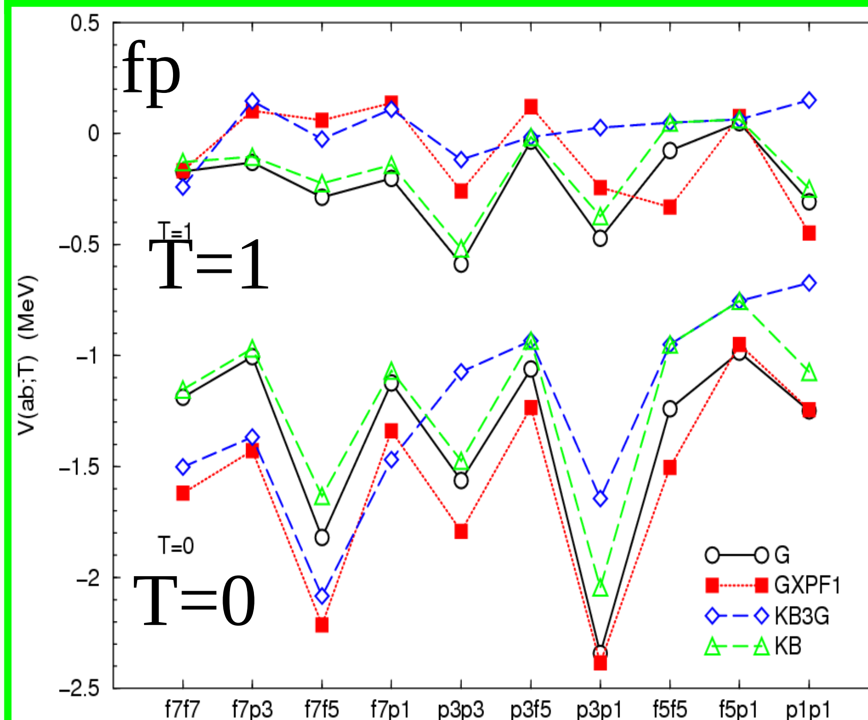

- **Modification of SFO**

Full inclusion of tensor force

·p-sd: tensor->π+ρ

LS -> σ+ρ+ω

$$V = V_C + V_T + V_{LS}$$

$$V_T = V_\pi + V_\rho$$

$$V_{LS} = V_{\sigma+\omega+\rho}$$

·sd: Kuo G-matrix

T=1 monopole terms more repulsive

→ SFO-tls

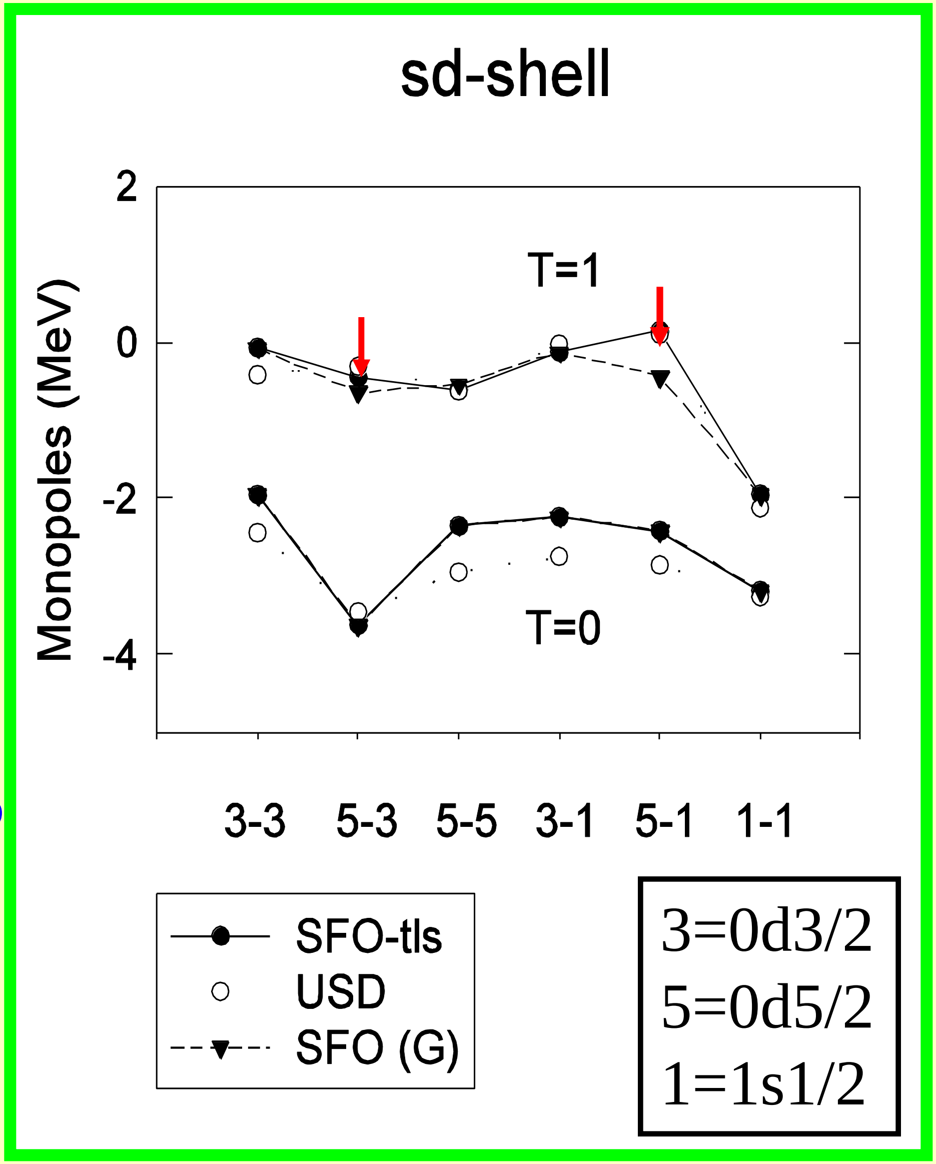

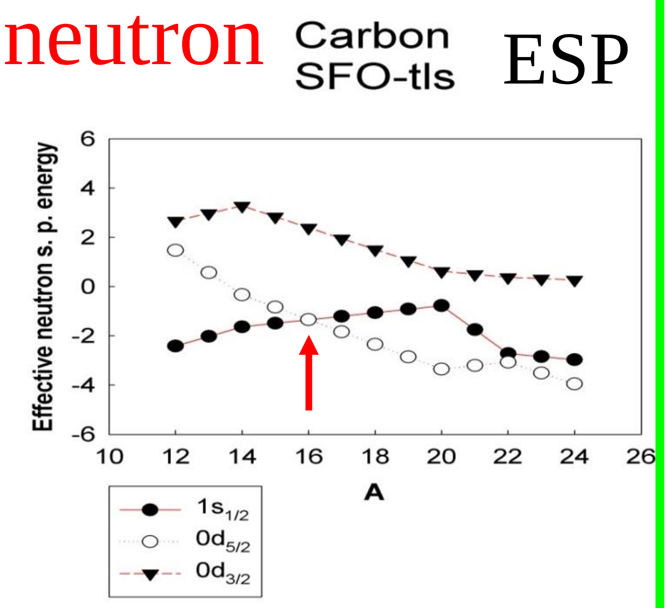

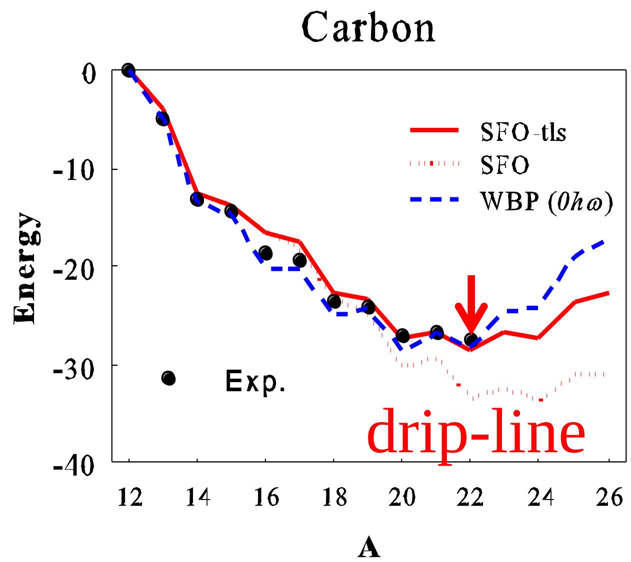

$Note$: ^{17}C

$d_{5/2}1s_{1/2} - space$

$|1/2^+ >=| d_{5/2}{}^2(0^+) \times 1s_{1/2} >$

$\nu d_{5/2}{}^3 \to 3/2^+, 5/2^+, 9/2^+$

$|3/2^+ >=| d_{5/2}{}^2(2^+) \times 1s_{1/2} >$

$| d_{5/2}{}^2(2^+, 4^+) \times d_{5/2} >$

$B(M1: 1/2^+ \to 3/2^+) = 0$

Anomalous suppression of B(M1) strength in ^{17}C

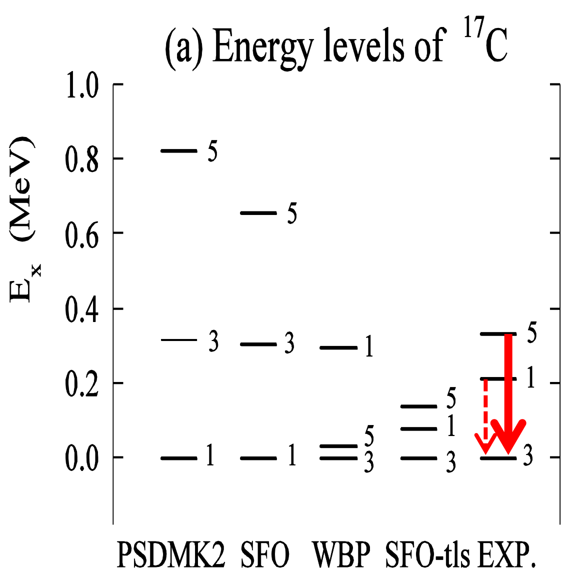

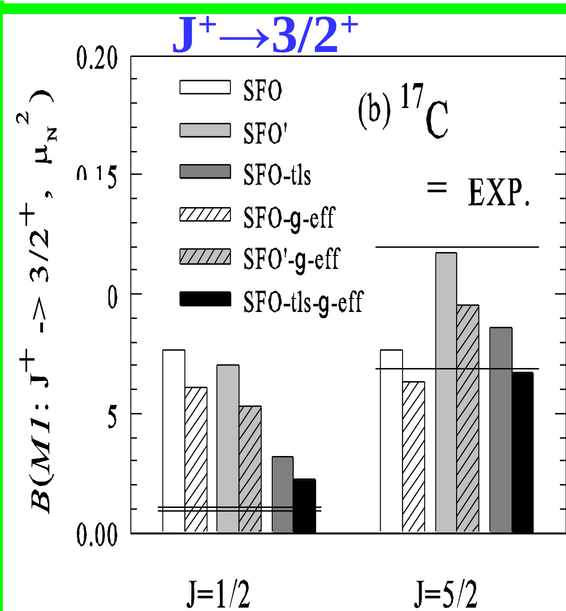

^{19}C: B(M1: $3/2^+ \to 1/2^+$) suppressed
Iwasaki et al., MSU

$|1/2^+\rangle = |d_{5/2}{}^4(0^+) \times 1s_{1/2}: 1/2^+\rangle$

$|3/2^+\rangle = \alpha\, |d_{5/2}{}^3(3/2^+) \times 1s_{1/2}{}^2(0^+): 3/2^+\rangle + \beta\, |d_{5/2}{}^4(2^+) \times 1s_{1/2}: 3/2^+\rangle$

$\langle 3/2^+ \| M1 \| 1/2^+\rangle = 0$

EXP: D. Suzuki et al., PLB666 (2008)

● Roles of three-body force on shell evolutions

three-body force = FM (Fujita-Miyazawa)

Δ-excitation by two-pion exchange

FM → repulsion between valence neutrons (T=1)

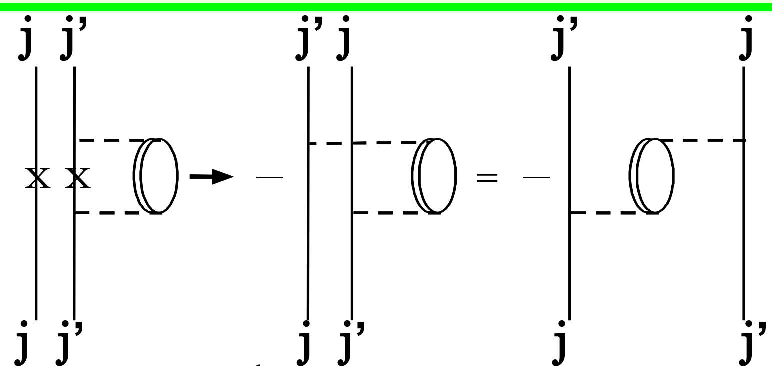

$$\frac{1}{\Delta E}\,|\langle pj'\,|\,V\,|\,hj\rangle|^2 > 0$$

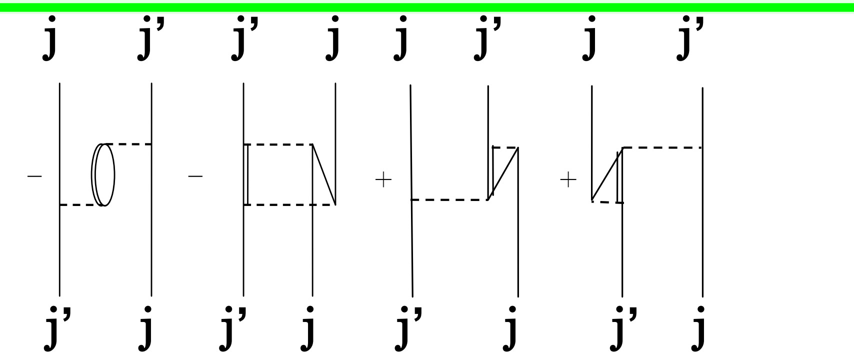

$$\frac{1}{\Delta E}\,|\langle pj\,|\,V\,|\,hj' - j'h\rangle|^2$$

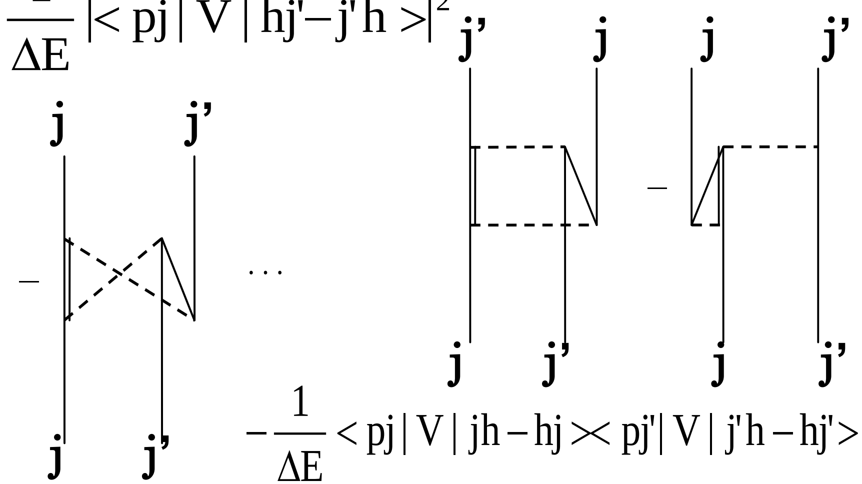

$$-\frac{1}{\Delta E}\langle pj\,|\,V\,|\,jh - hj\rangle\langle pj'\,|\,V\,|\,j'h - hj'\rangle$$

$$\frac{1}{\Delta E}\,|\langle ph\,|\,V\,|\,jj' - j'j\rangle|^2$$

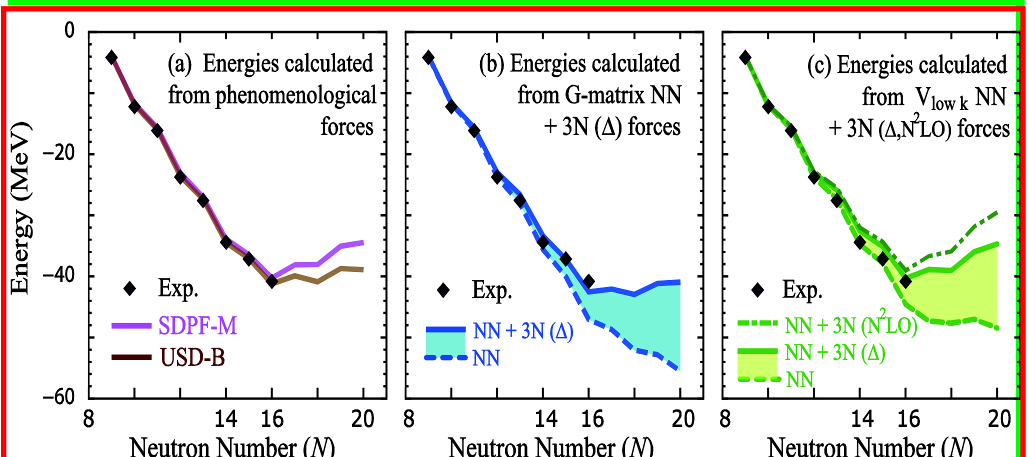

Oxgen isotopes: drip-line at ^{24}O

Otsuka, Suzuki, Holt, Schwenk, Akaishi, PRL 105 (2010)

pf-shell **ESPE** **Energies of Ca isotopes** **E (2^+)**

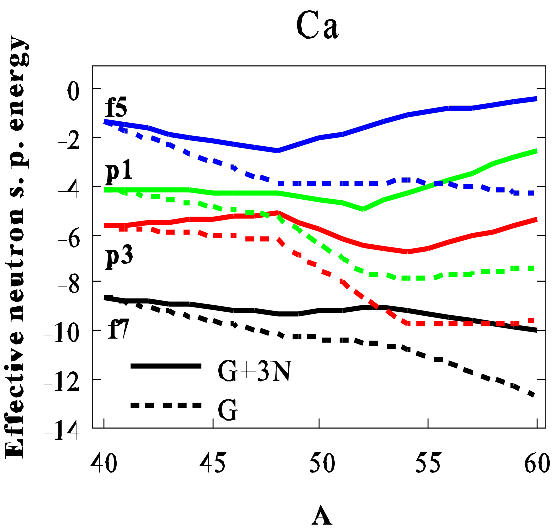

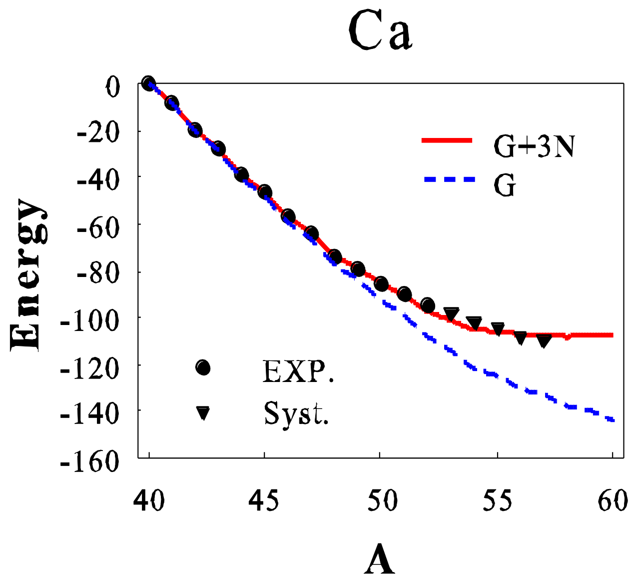

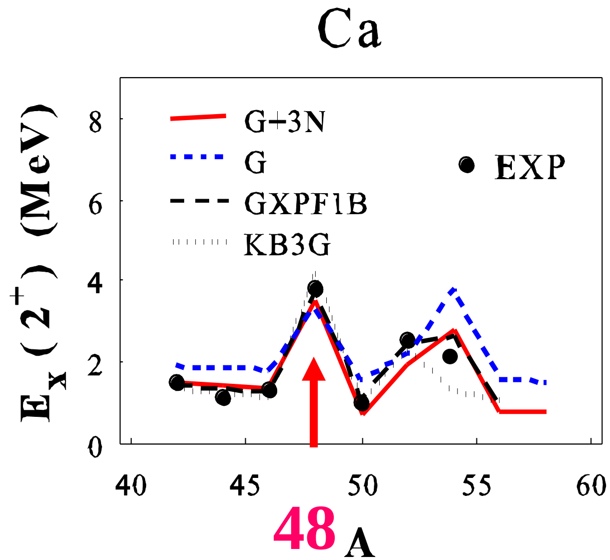

G-matrix; 3rd Q-box up to 24 hw excitations
Hjorth-Jensen

3-body force →repulsion

shell-closure at A=48

^{48}Ca B(M1)
+3N →
concentration of the strength

EXP.: Steffen et al.
NP A404, 413 (1983)

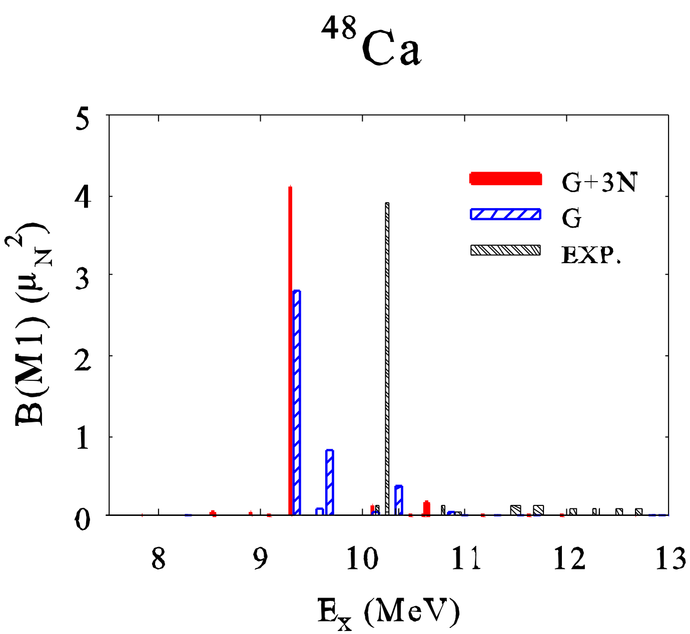

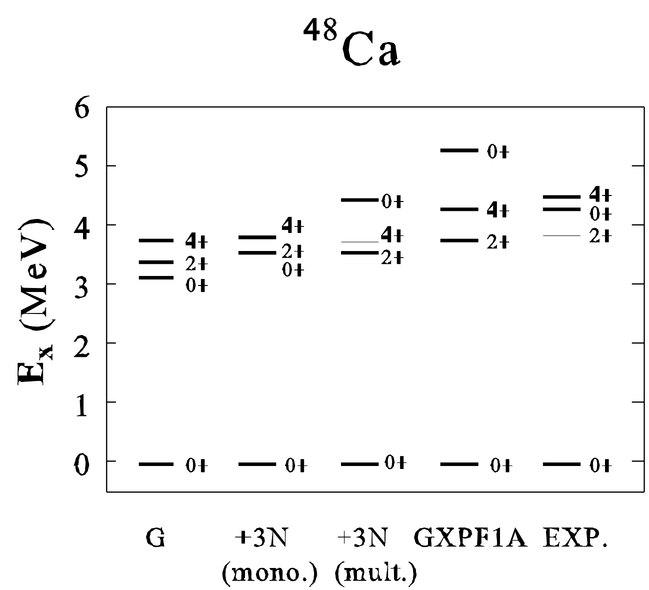

pf-$g_{9/2}$ shell

degenerate pf-$g_{9/2}$ orbits

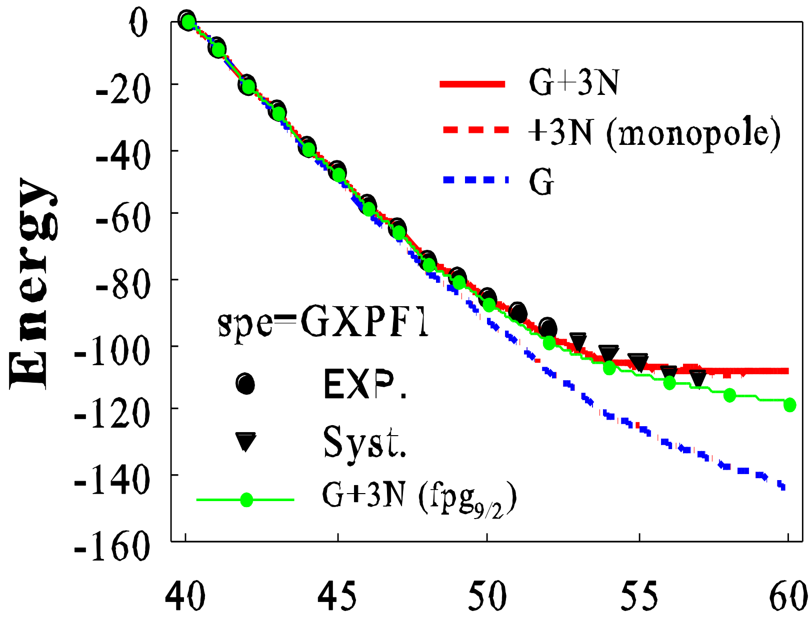

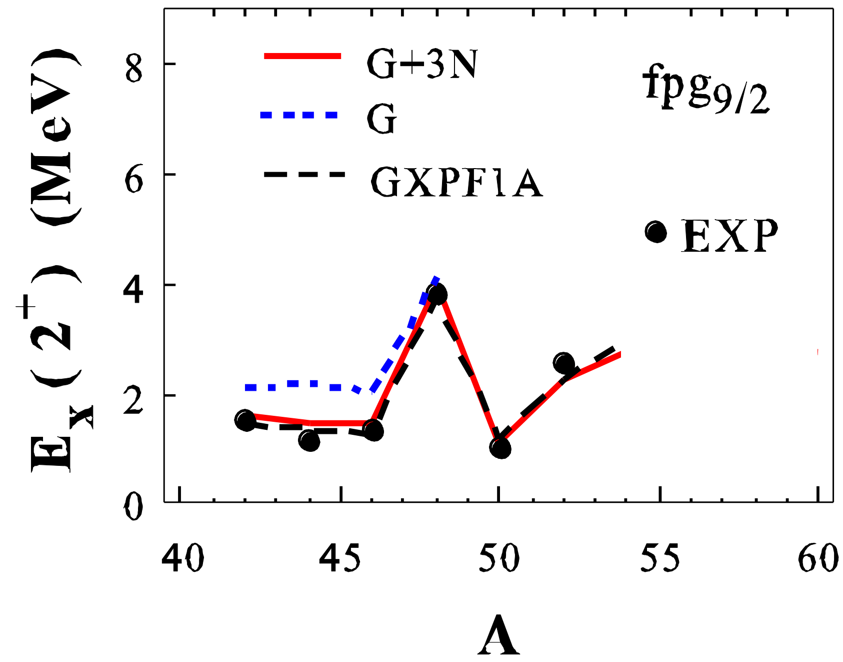

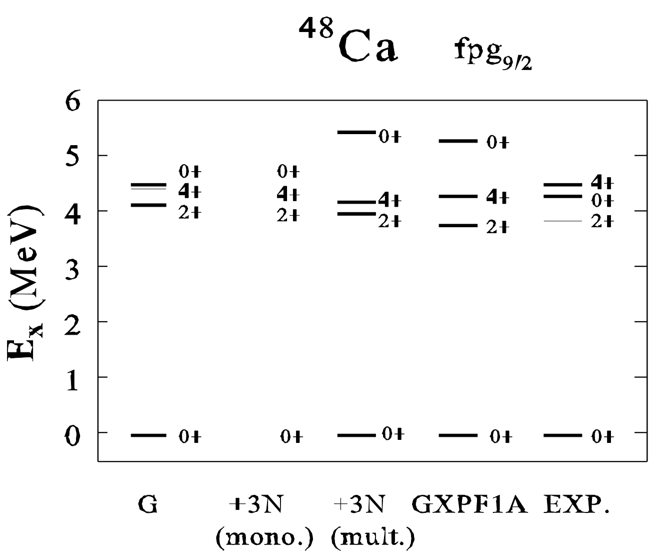

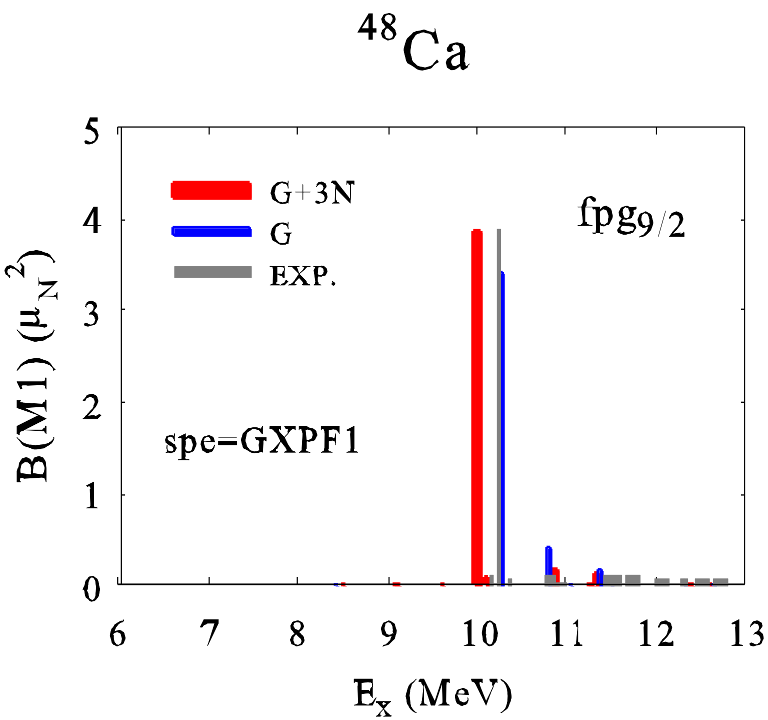

pf-$g_{9/2}$ shell

Non-degenerate treatment of pf and $g_{9/2}$ shells by
EKK (extended Kuo-Krenciglowa) method

Tsunoda, Takayanagi, Hjorth-Jensen and Otsuka, Phys. Rev. C 89, 024313 (2014)

Cf: monopoles with non-degenerate vs degenerate method

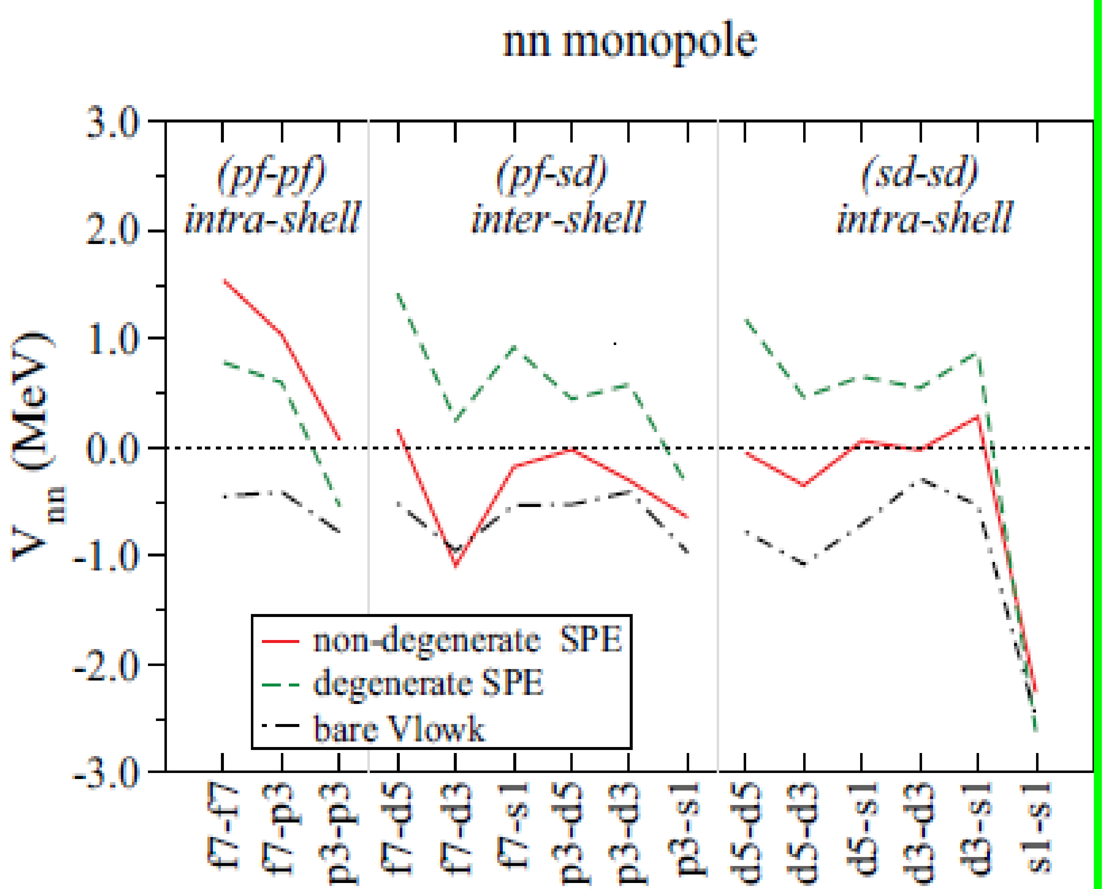

Kuo-Krenciglowa method

$$V_{\rm eff}^{(n)} = \hat{Q}(\epsilon_0) + \sum_{k=1}^{\infty} \hat{Q}_k(\epsilon_0)\{V_{\rm eff}^{(n-1)}\}^k,$$

$$PH_0P = \epsilon_0 P.$$

$$\hat{Q}(E) = PVP + PVQ\frac{1}{E-QHQ}QVP,$$

$$\hat{Q}_k(E) = \frac{1}{k!}\frac{d^k\hat{Q}(E)}{dE^k}.$$

Extended Kuo-Krenciglowa method

$$\tilde{H} = H - E$$

$$\tilde{H}_{\rm eff}^{(n)} = \tilde{H}_{\rm BH}(E) + \sum^{\infty} \hat{Q}_k(E)\{\tilde{H}_{\rm eff}^{(n-1)}\}^k,$$

$$\tilde{H}_{\rm eff} = H_{\rm eff} - E, \quad \tilde{H}_{\rm BH}(E) = H_{\rm BH}(E) - E,$$

$$H_{\rm BH}(E) = PHP - PVQ\frac{1}{E-QHQ}QVP.$$

$$V_{\rm eff} = H_{\rm eff} - PH_0P.$$

energy indpendent

K. Takayanagi, Nucl. Phys. A **852**, 61 (2011).
K. Takayanagi, Nucl. Phys. A **864**, 91 (2011).

Ground state energies & E(2_1^+)

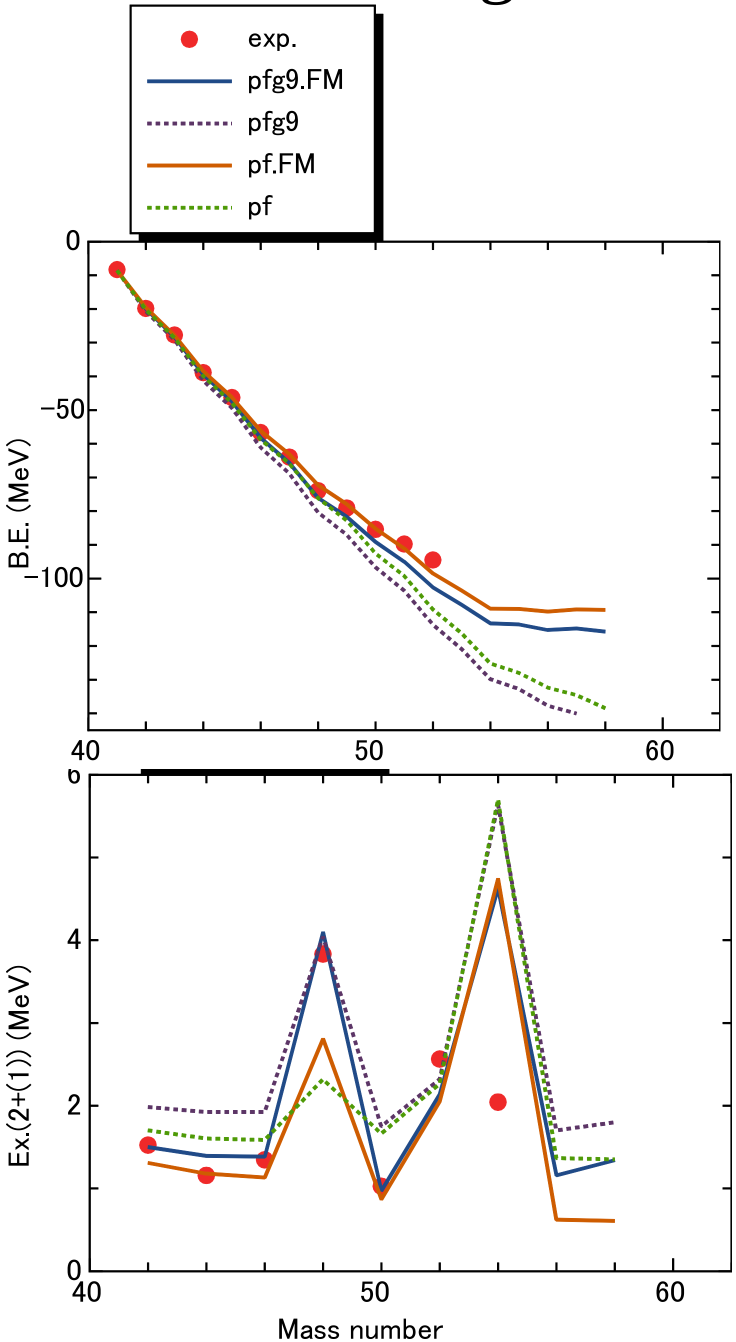

^{48}Ca
B(M1)

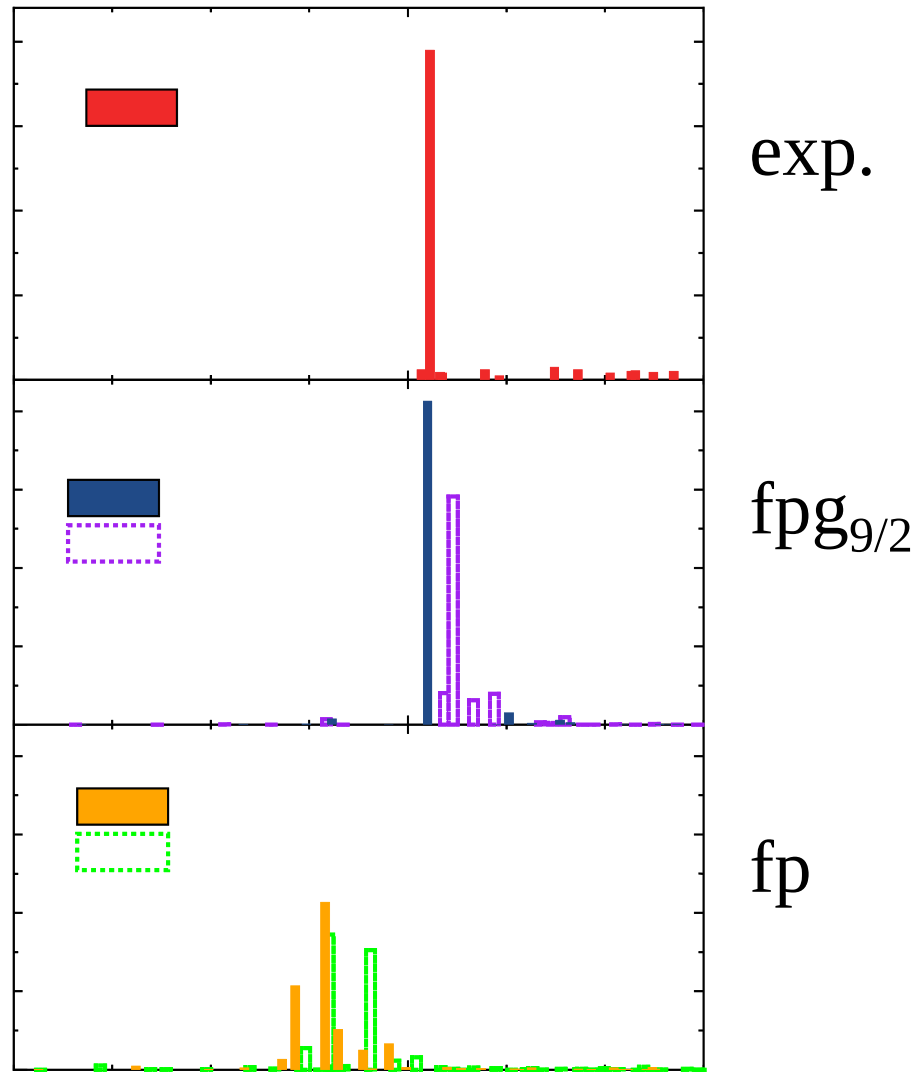

Tsunoda, Shimizu

cf. Holt et al., J. Phys. G39, 085111 (2012)

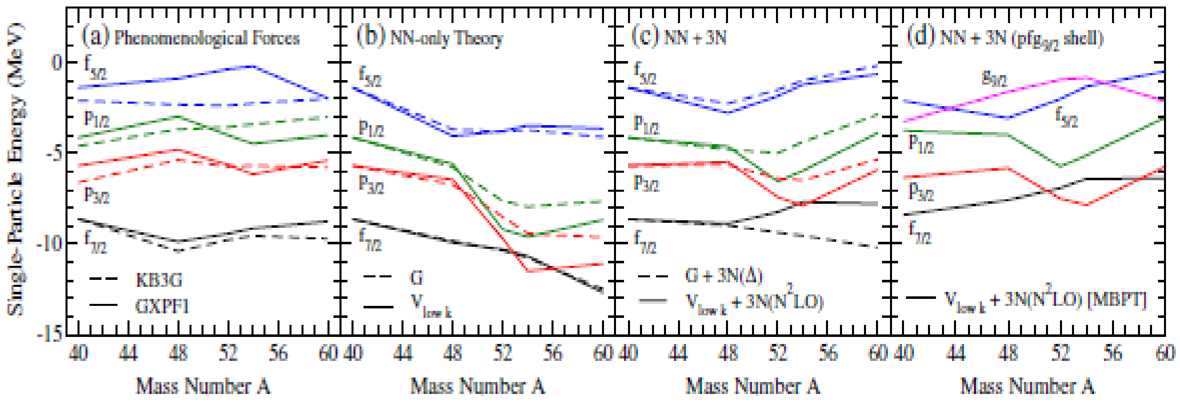

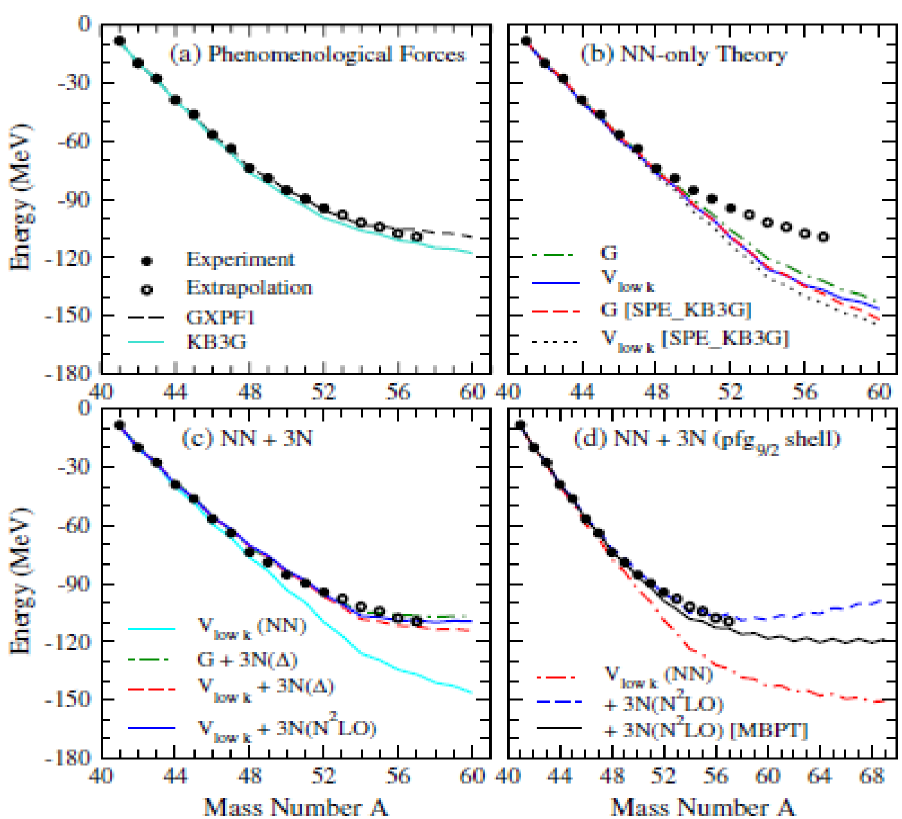

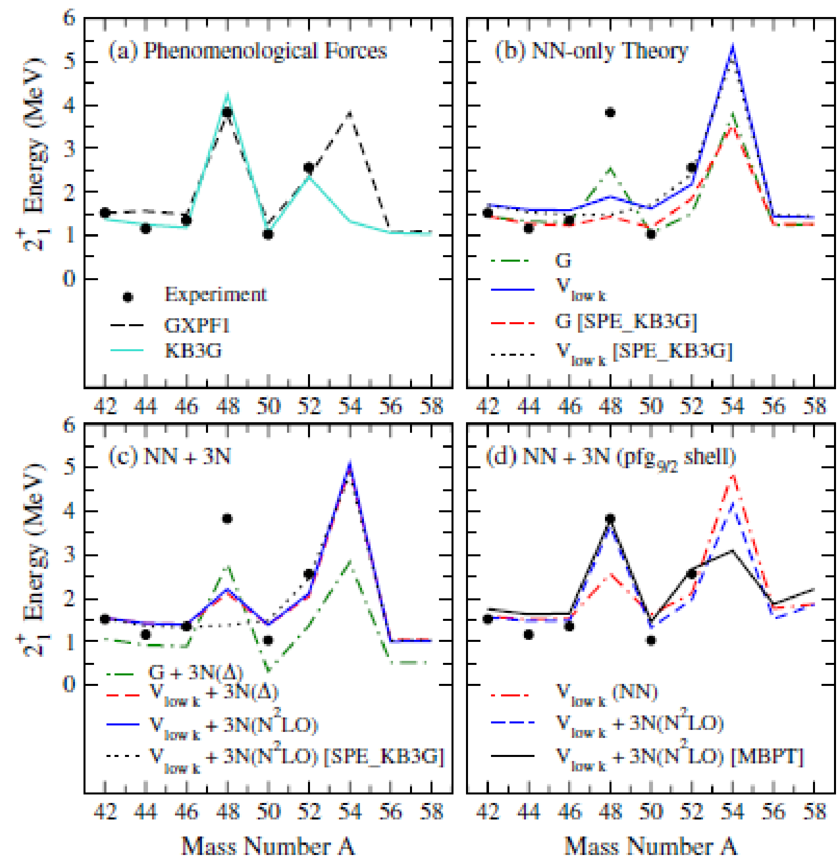

Summary

- **New spin-dependent transition strengths based on new shell-model Hamiltonians with proper tensor forces (SFO for p-shell, GXPF1 for pf-shell, VMU)**

- **Good reproduction of experimental B(GT) in ^{12}C, ^{56}Fe and ^{56}Ni and cross section data for ν-induced reactions on ^{12}C and ^{56}Fe**

- **Light element synthesis in SN explosions and effects of ν-oscillations (MSW effects) in nucleosynthesis**
  Abundance ratio of $^{7}Li/^{11}B$ → ν mass hierarchy

- **GXPF1J well describes the GT strengths in Ni isotopes :**
  ^{56}Ni two-peak structure confirmed by recent exp.

→ Accurate evaluation of e-capture rates at stellar environments
Implications on synthesis of Ni isotopes; $^{58}Ni/^{56}Ni$

- **VMU for ^{40}Ar (sd-pf-shell) and p-sd shell nuclei:**
  GT strength consistent with observations
  New cross section for $^{40}Ar(\nu,e^-)^{40}K$ induced by solar ν
- **Detailed e-capture and beta-decay rates for URCA nuclear pairs in 8-10 solar-mass stars**
  → URCA density for A=25 and 23 with fine mesh of density and temperature
  → Cooling of O-Ne-Mg core by nuclear URCA processes determines the fate of the stars.
- **Repulsive contributions from FM three-nucleon forces in T=1 monopoles**
  → Shell evolutions in neutron-rich isotopes
  Ca: shell-closure at ^{48}Ca and M1 strength
  pf vs pf-$g_{9/2}$ by non-degenerate treatment of $g_{9/2}$

Collaborators

T. Otsuka[a], M. Honma[b], N. Tsunoda[c], N. Shimizu[a]
T. Kajino [d], S. Chiba[e], T. Yoshida[f]

[a]CNS and Dept. of Physisc, the Univ. of Tokyo
[b]University of Aizu
[c]the University of Tokyo
[d]National Astronomical Observatory of Japan
Department of Astronomy, the University of Tokyo
[e]Tokyo Institute of Technology
[f]YITP, Kyoto University

Collaborators

H. Toki[g], K. Nomoto[h], S. Jones[i], R. Hirsci[i]
A. Balantekin[j]

[g]RCNP, Osaka University
[h]WPI, the Univ. of Tokyo
[i]Keele University, [j]RIKEN
[j]Univ. of Wisconsin